Spin Hall Effect

Guang-Yu Guo (郭光宇)

Physics Dept, National Taiwan University, Taiwan

(國立臺灣大學物理系)

(A Colloquium Talk in Department of Physics,

National Taiwan University, 22 April 2014)

Plan of this Talk

I. Introduction, overview and outlook
   1. What is spin Hall effect
   2. Spin Hall effect observed in semiconductors
   3. Large room-temperature spin Hall effect in metals
   4. Spintronics, magneto-electric devices and spin Hall effect
   5. Spin-off's: Topological insulators and spin caloritronics

II. *Ab initio* calculation of intrinsic spin Hall effect in solids
   1. Motivations
   2. Berry phase formalism for intrinsic Hall effects.
   3. Intrinsic spin Hall effect in platinum

III. Gigantic spin Hall effect in gold and multi-orbital Kondo effect
   1. Gigantic spin Hall effect in gold/FePt
   2. Spin Hall effect enhanced by multi-orbital Kondo effect.
   3. Quantum Monte Carlo simulation

IV. Summary

I. Introduction, overview and outlook

1. What is spin Hall effect

1) Ordinal Hall Effect

Lorentz force

$q\mathbf{v}\times\mathbf{B}$

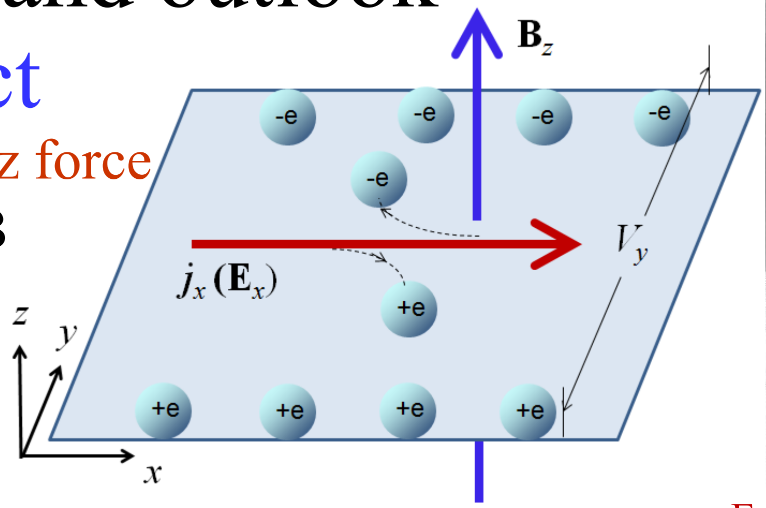

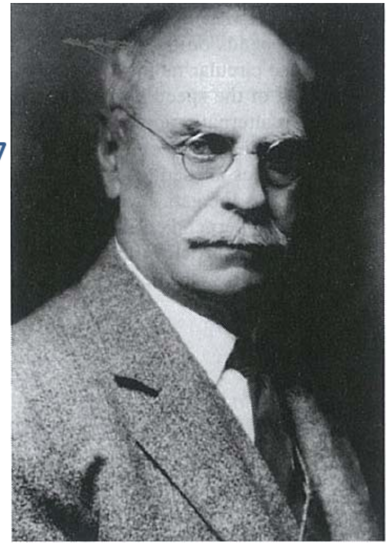

Edwin H. Hall (1855-1938)

[Hall 1879]

$$\rho_{\text{Hall}} = R_0 B$$

2) Anomalous Hall Effect [Hall, 1880 & 1881]

$$\rho_{\text{Hall}} = R_0 B + R_S M$$

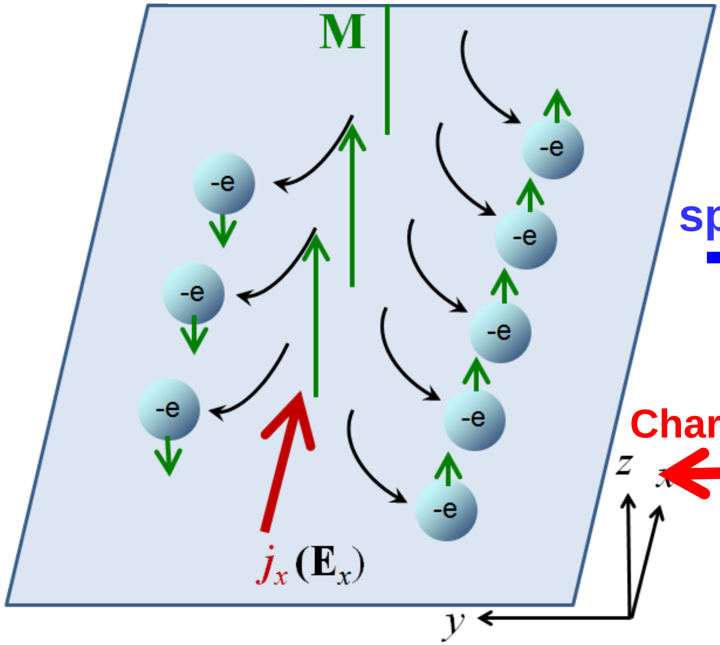

spin current

Charge current

Spin-orbit interaction

$$\frac{dV(r)}{dr}(\mathbf{s}\cdot\mathbf{L})$$

(Mott or skew scattering)

3) Extrinsic spin Hall Effect

[Dyakonov & Perel, JETP 1971]

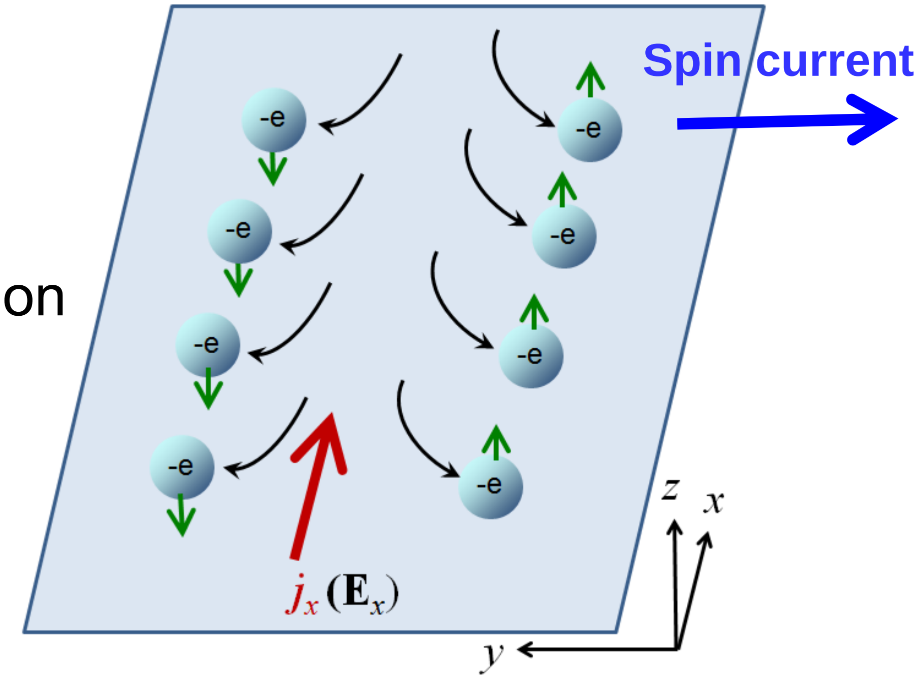

4) Intrinsic spin Hall effect

(1) In p-type zincblende semiconductors

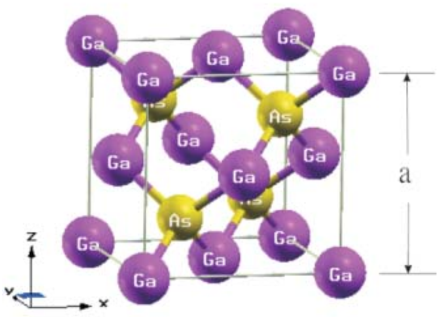

[Science 301, 1348 (2003)]

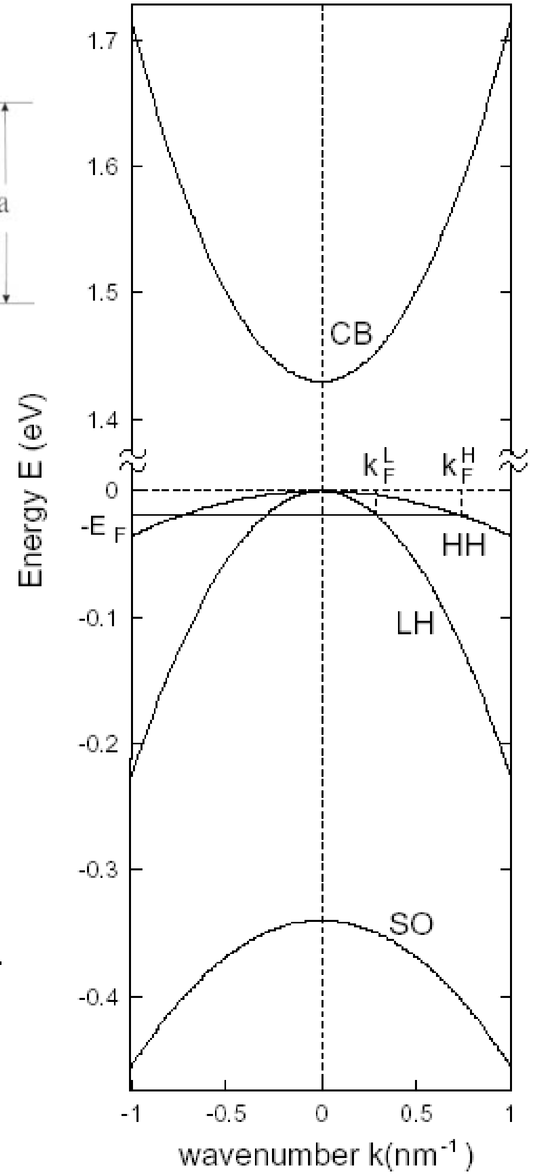

Dissipationless Quantum Spin Current at Room Temperature

Shuichi Murakami,[1*] Naoto Nagaosa,[1,2,3] Shou-Cheng Zhang[4]

Luttinger model
$$H_0 = \frac{\hbar^2}{2m}\left[(\gamma_1 + \frac{5}{2}\gamma_2)k^2 - 2\gamma_2(\vec{k}\cdot\vec{S})^2\right]$$

Dirac monopole
$$F_{ij} \equiv i[D_i, D_j] = \epsilon_{ijk}\lambda\frac{k_k}{k^3}$$

Equation of motion
$$\left\langle \dot{X}_i \right\rangle = \frac{\hbar k_i}{m_\lambda} + F_{il}\left\langle \dot{k}_l \right\rangle$$

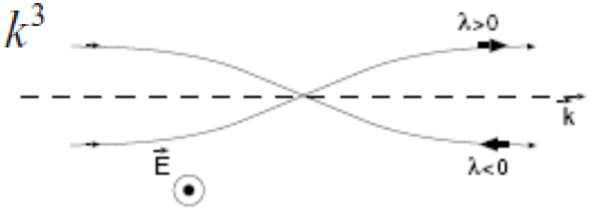

$$\left\langle \dot{k}_i \right\rangle = \frac{e}{\hbar}E_i \quad e > 0 \text{ (hole)}$$

Anomalous velocity
$$\left\langle \dot{\vec{X}} \right\rangle = \frac{\hbar\vec{k}}{m_\lambda} - \frac{e\lambda}{\hbar k^3}\vec{k}\times\vec{E}$$

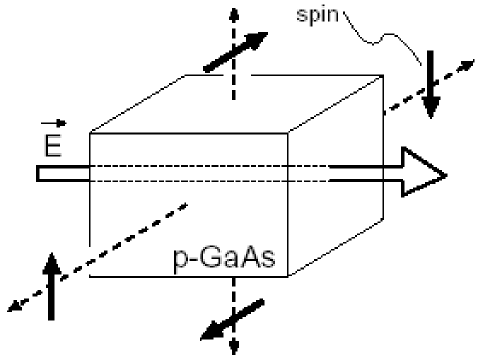

$$j_j^i = \sigma_s \varepsilon^{ijk} E_k$$

$$j_y^x = \frac{eE_z}{12\pi^2}(3k_F^H - k_F^L) = \frac{\hbar}{2e}\sigma_s E_z$$

$n_h = 10^{19}$ cm^{-3}, μ= 50 cm /V·s, $\sigma = e\mu n_h$ = 80 Ω^{-1}cm^{-1};
σ_s= 80 Ω^{-1}cm^{-1}

$n_h = 10^{16}$ cm^{-3}, μ= 50 cm /V·s, $\sigma = e\mu n_h$ = 0.6 Ω^{-1}cm^{-1};
σ_s= 7 Ω^{-1}cm^{-1}

(2) In a 2-D electron gas in n-type semiconductor heterostructures

Universal Intrinsic Spin Hall Effect

[PRL 92, 126603]

Jairo Sinova,[1,2] Dimitrie Culcer,[2] Q. Niu,[2] N. A. Sinitsyn,[1] T. Jungwirth,[2,3] and A. H. MacDonald[2]

Rashba Hamiltonian

$$H = \frac{p^2}{2m} - \frac{\lambda}{\hbar}\vec{\sigma}\cdot(\hat{z}\times\vec{p}), \qquad (1)$$

contributes to the spin current. In this case we find that the spin current in the $\hat{y}$ direction is [23]

$$j_{s,y} = \int_{\text{annulus}} \frac{d^2\vec{p}}{(2\pi\hbar)^2}\frac{\hbar n_{z,\vec{p}}}{2}\frac{p_y}{m} = \frac{-eE_x}{16\pi\lambda m}(p_{F+} - p_{F-}), \qquad (6)$$

where p_{F+} and p_{F-} are the Fermi momenta of the majority and minority spin Rashba bands. We find that when both bands are occupied, i.e., when $n_{2D} > m^2\lambda^2/\pi\hbar^4 \equiv n_{2D}^*$, $p_{F+} - p_{F-} = 2m\lambda/\hbar$ and then the spin Hall (sH) conductivity is

Universal spin Hall conductivity

$$\sigma_{sH} \equiv -\frac{j_{s,y}}{E_x} = \frac{e}{8\pi}, \qquad (7)$$

independent of both the Rashba coupling strength and of the 2DES density. For $n_{2D} < n_{2D}^*$ the upper Rashba band is depopulated. In this limit p_{F-} and p_{F+} are the interior and exterior Fermi radii of the lowest Rashba split band, and σ_{sH} vanishes linearly with the 2DES density:

$$\sigma_{sH} = \frac{e}{8\pi}\frac{n_{2D}}{n_{2D}^*}. \qquad (8)$$

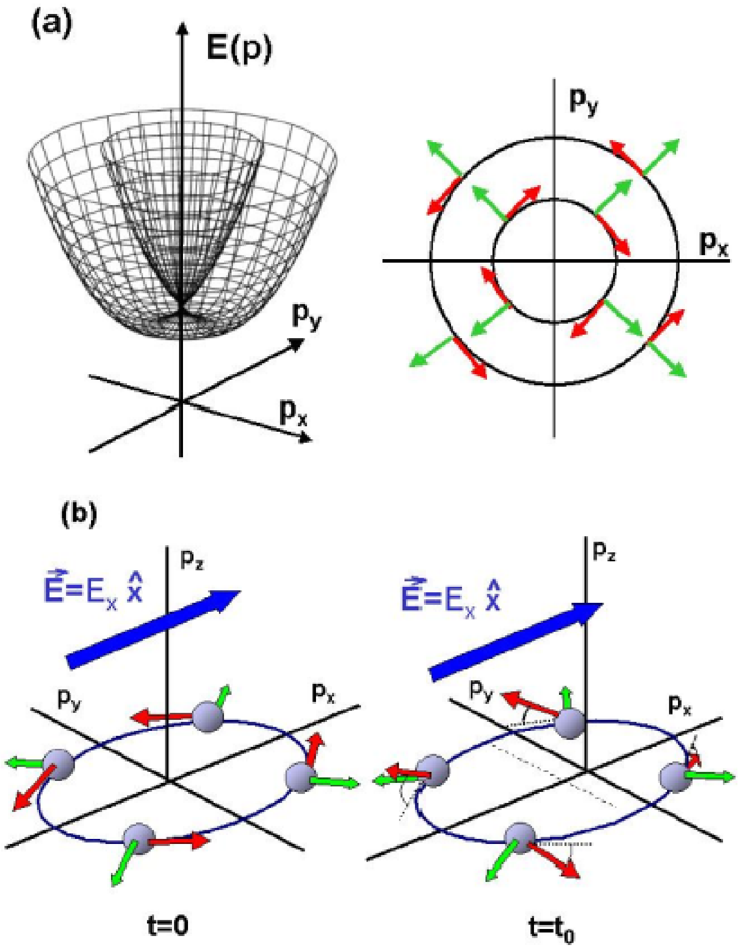

2. Spin Hall effect observed in semiconductors

(a) in n-type 3D GaAs and InGaAs thin films

[Kato *et al.*, Science 306, 1910 (2004)]

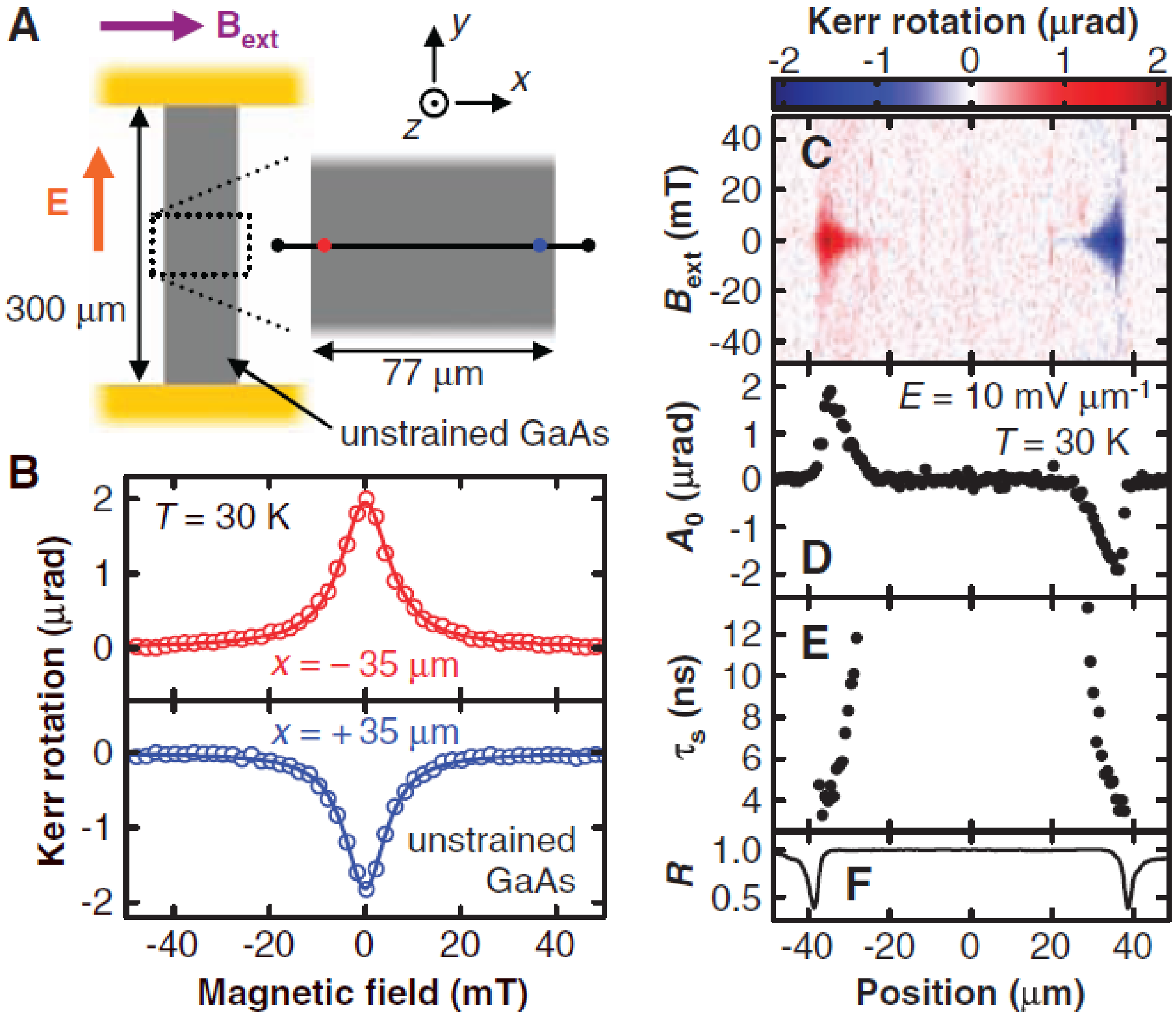

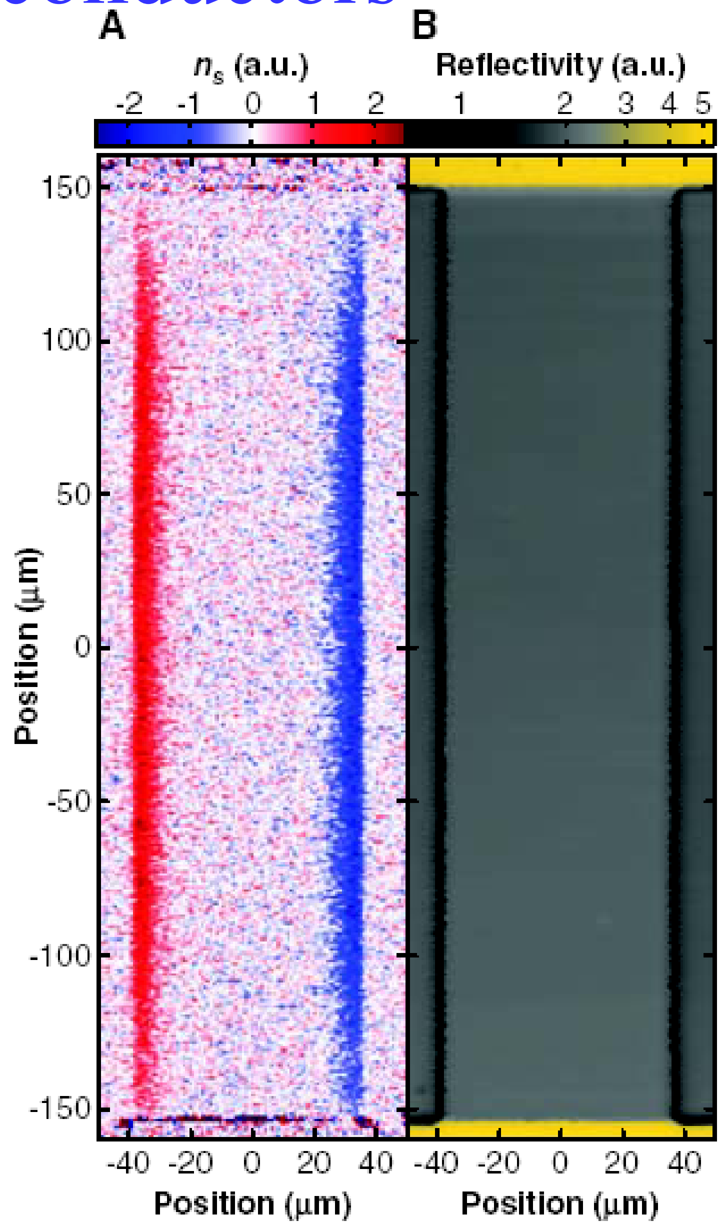

Fig. 2. (**A** and **B**) Two-dimensional images of spin density n_s and reflectivity R, respectively, for the unstrained GaAs sample measured at T = 30 K and E = 10 mV μm^{-1}.

Attributed to extrinsic SHE because of weak crystal direction dependence.

(b) in p-type 2D semiconductor quantum wells

Experimental Observation of the Spin-Hall Effect in a Two-Dimensional Spin-Orbit Coupled Semiconductor System

[PRL 94 (2005) 047204]

J. Wunderlich,[1] B. Kaestner,[1,2] J. Sinova,[3] and T. Jungwirth[4,5]

We report the experimental observation of the spin-Hall effect in a 2D hole system with spin-orbit coupling. The 2D hole layer is a part of a *p*-*n* junction light-emitting diode with a specially designed coplanar geometry which allows an angle-resolved polarization detection at opposite edges of the 2D hole system. In equilibrium the angular momenta of the spin-orbit split heavy-hole states lie in the plane of the 2D layer. When an electric field is applied across the hole channel, a nonzero out-of-plane component of the angular momentum is detected whose sign depends on the sign of the electric field and is opposite for the two edges. Microscopic quantum transport calculations show only a weak effect of disorder, suggesting that the clean limit spin-Hall conductance description (intrinsic spin-Hall effect) might apply to our system.

Attributed to intrinsic SHE.

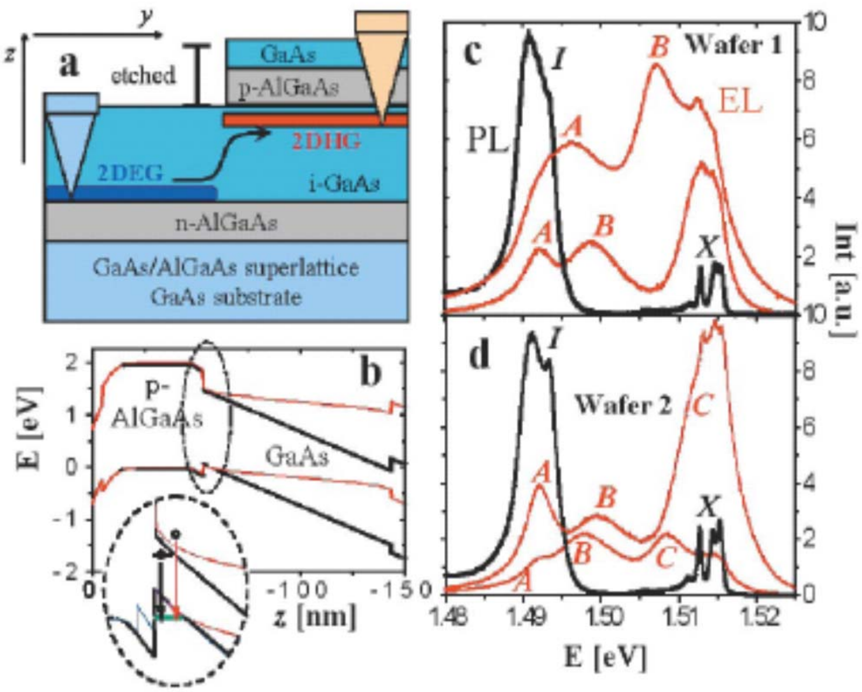

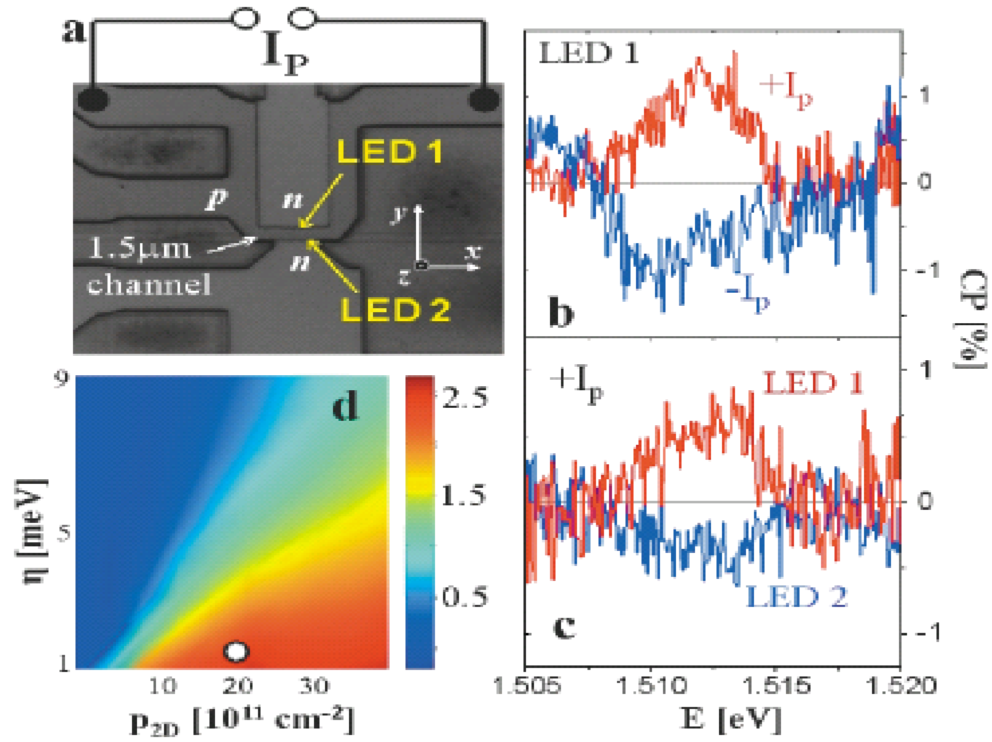

(c) Spin Hall effect in strained *n*-type nitride semiconductors

[Chang, Chen, Chen, Hong, Tsai, Chen, Guo, PRL 98, 136403; 98, 239902 (E) (2007)]

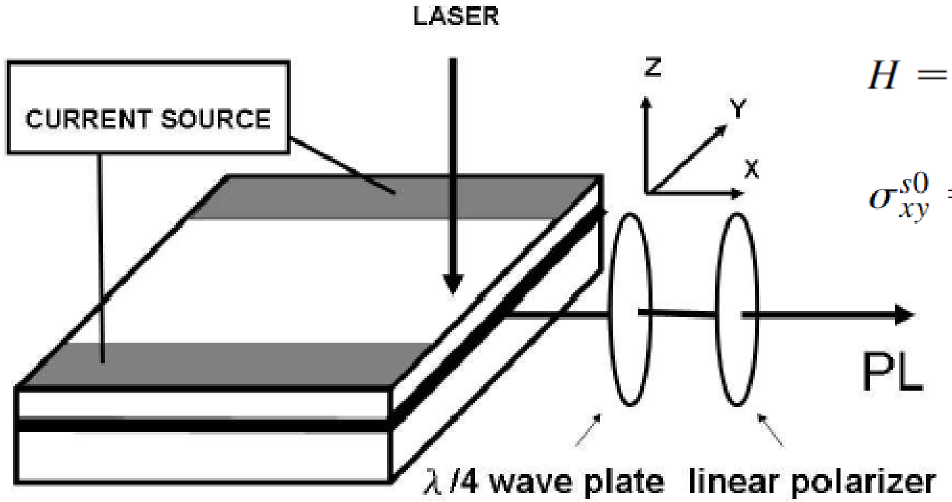

$$H = \frac{\hbar k^2}{2m} + (\alpha_e + \beta k^2)(\sigma_x k_y - \sigma_y k_x)$$

$$\sigma_{xy}^{s0} = -\sigma_{yx}^{s0} \approx \frac{e}{8\pi}\left[1 + \frac{2}{3}\alpha_e \beta\left(\frac{2m}{\hbar^2}\right)^2\right]$$

wurtzite

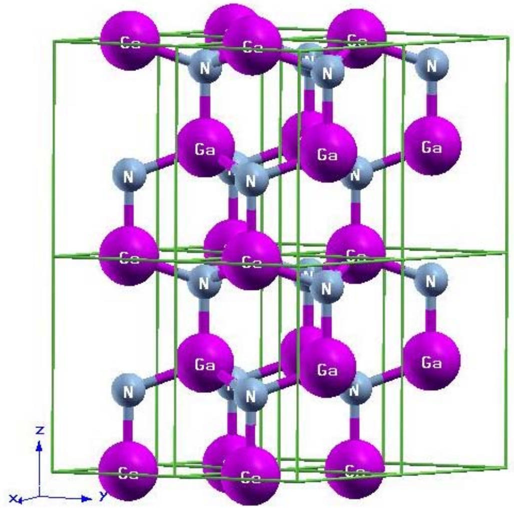

n-type (5nm $In_xGa_{1-x}N$/3nm GaN) superlattice (x=0.15)

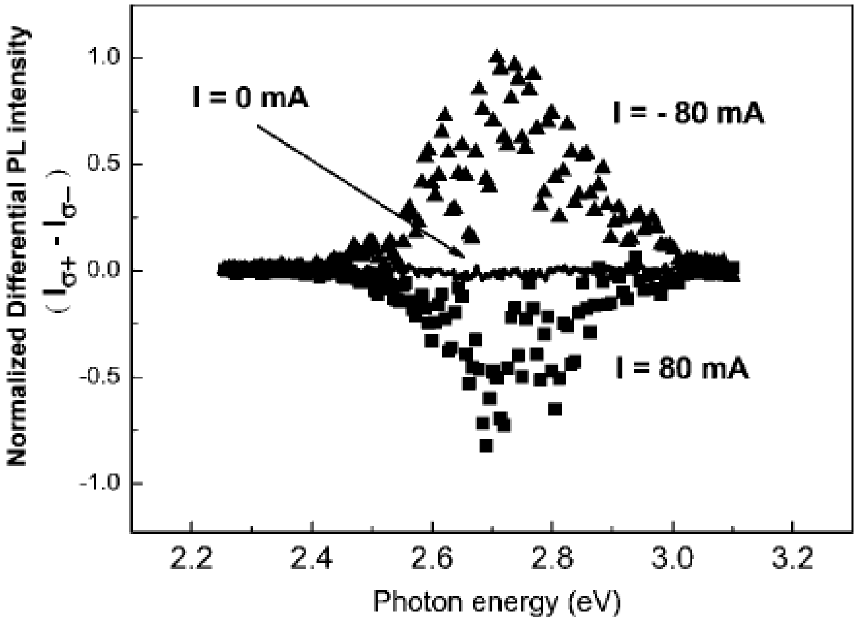

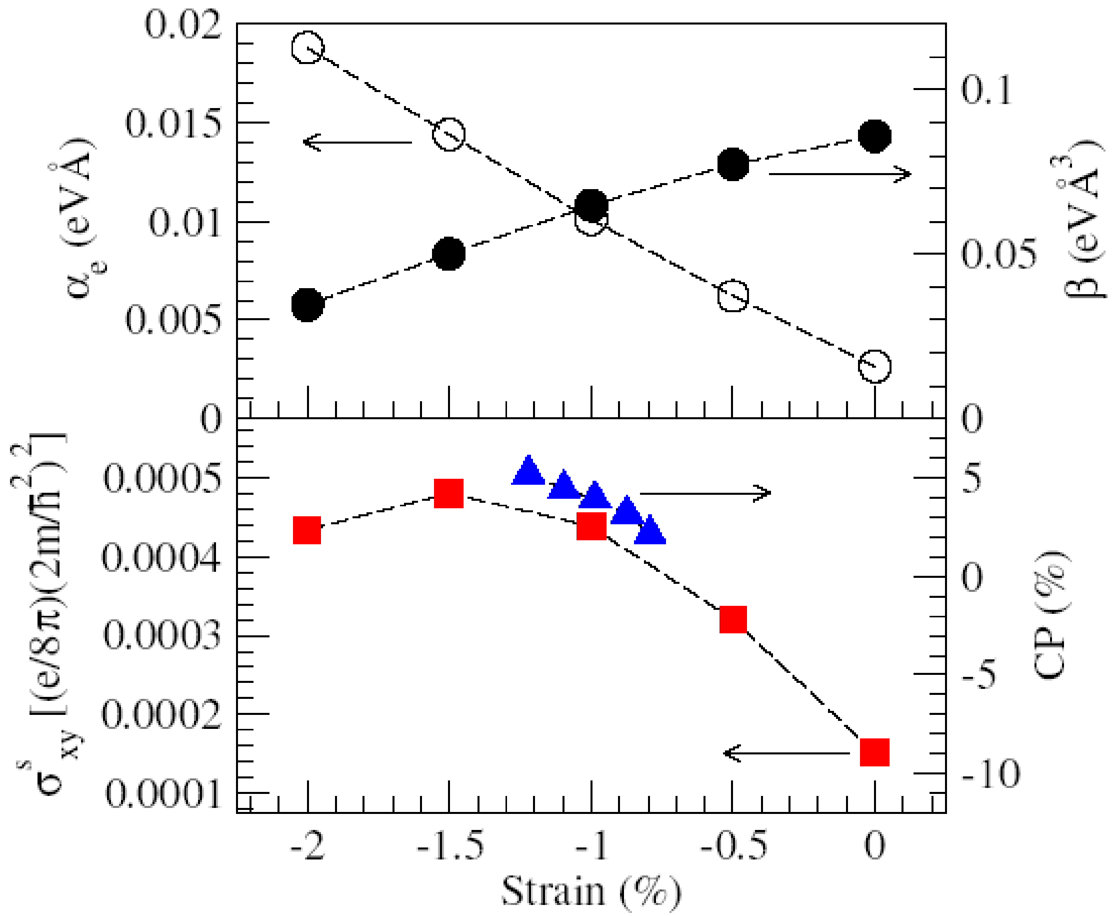

3. Large room-temperature spin Hall effect in metals

Nature 13 July 2006 Vol. 442, P. 176

Direct electronic measurement of the spin Hall effect fcc Al

S. O. Valenzuela[1]† & M. Tinkham[1]

$$R_{SH} = \frac{\Delta R_{SH}}{2} \sin\theta$$

$$\Delta R_{SH} = \frac{P}{t_{Al}} \frac{\sigma_{SH}}{\sigma_c^2} \exp(-L_{SH}/\lambda_{sf})$$

$\sigma_{sH} = 27\sim34\ (\Omega\text{cm})^{-1}$ (T= 4.2 K)

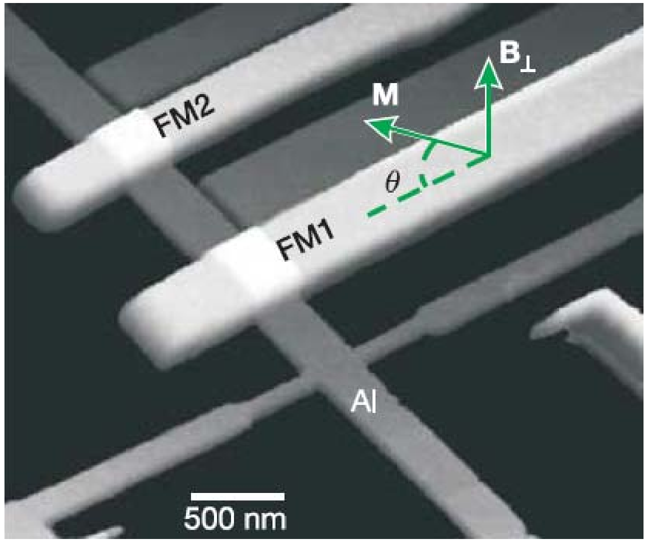

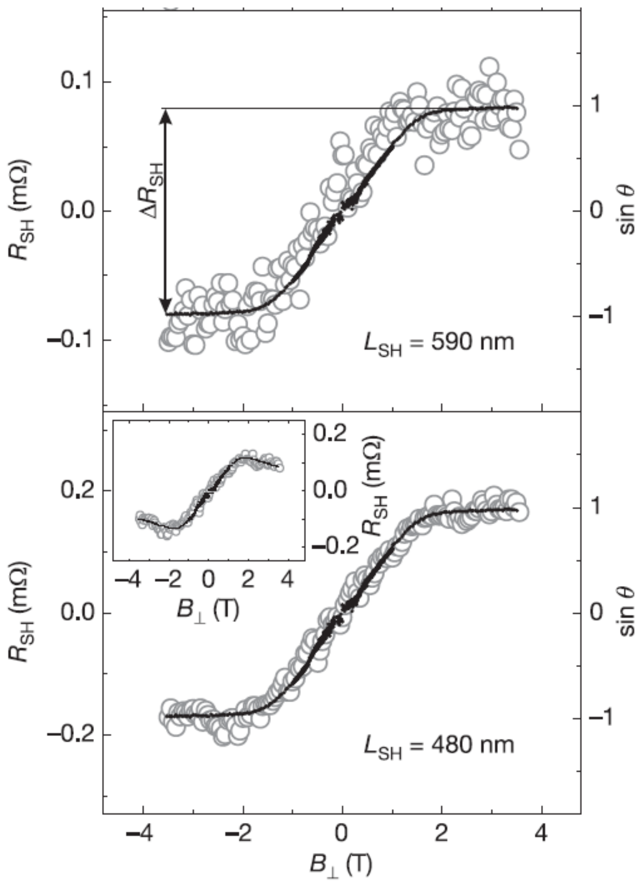

(direct) spin Hall effect

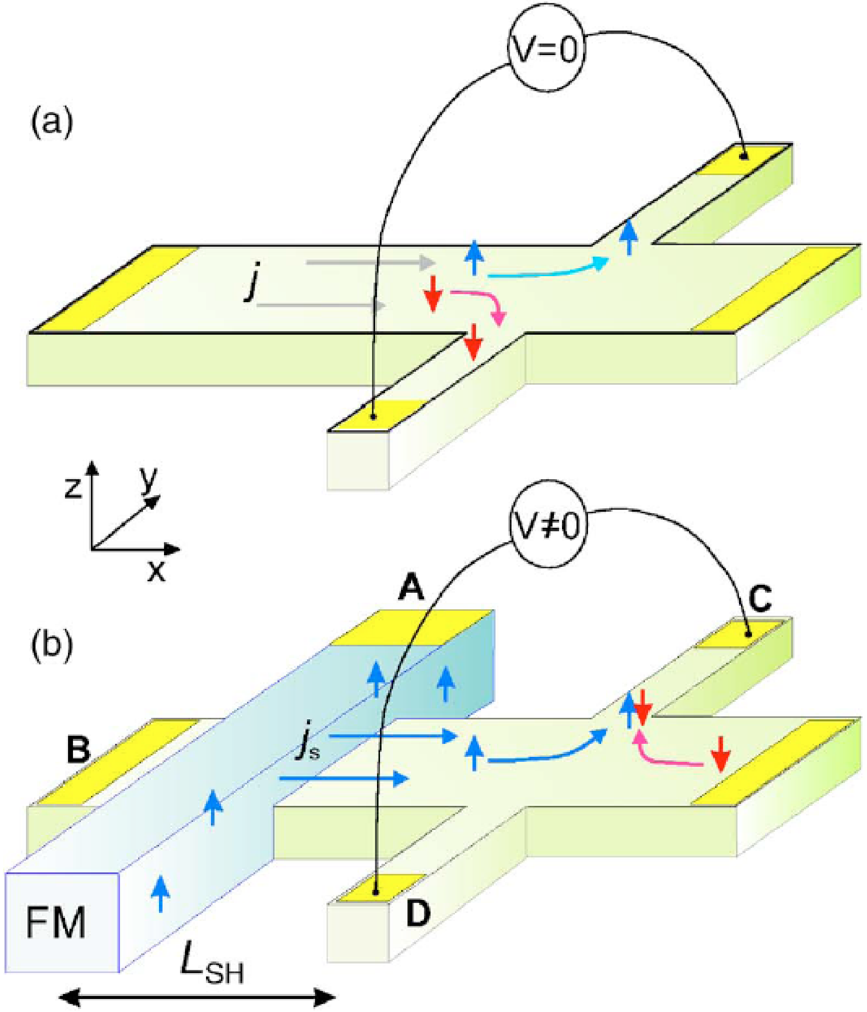

inverse spin Hall effect

Conversion of spin current into charge current at room temperature: Inverse spin-Hall effect

[Saitoh, et al.,
APL 88 (2006) 182509]

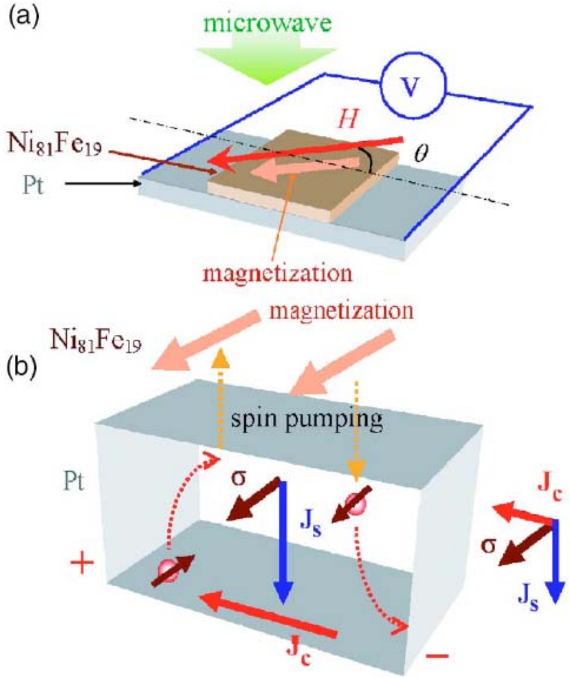

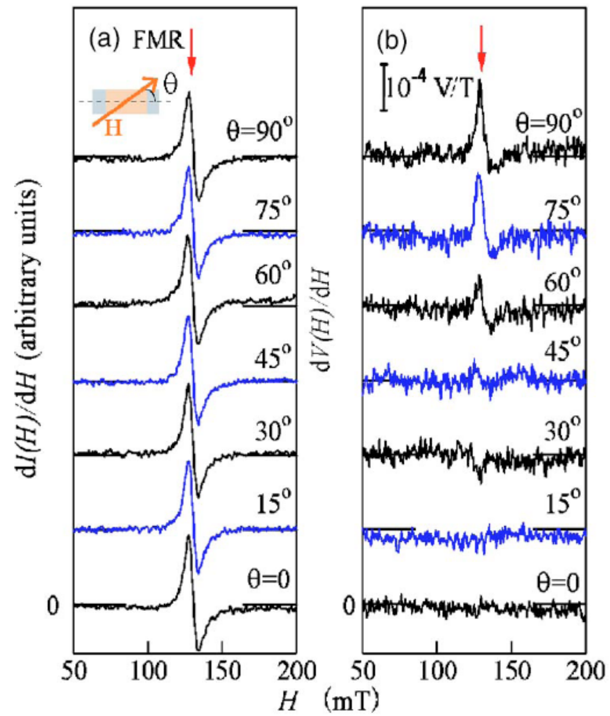

Room-Temperature Reversible Spin Hall Effect

[PRL98, 156601; 98, 139901 (E) (2007)]

T. Kimura,[1,2] Y. Otani,[1,2] T. Sato,[1] S. Takahashi,[3,4] and S. Maekawa[3]

$\sigma_{sH} = 240\ (\Omega\text{cm})^{-1}$
(T= 290 K)

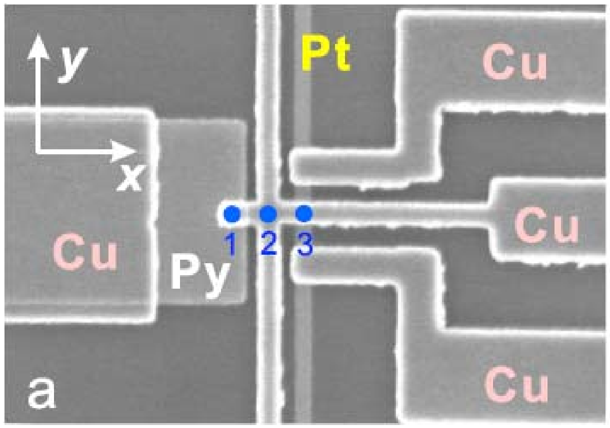

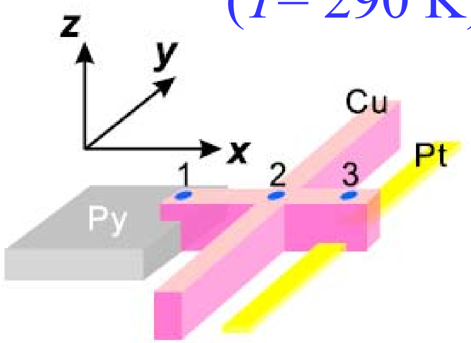

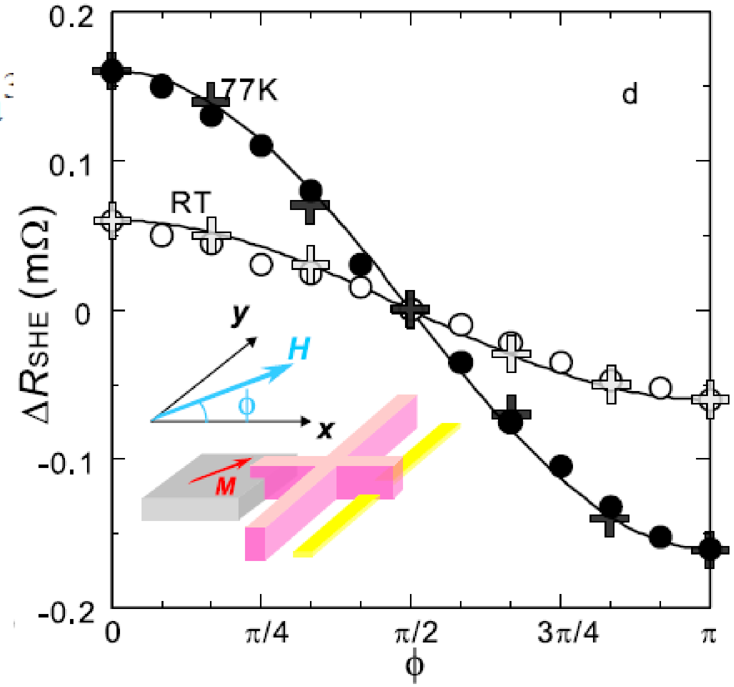

Assumed to be extrinsic!

Charge Conductivities, Spin Hall Conductivities, and Spin Hall Angles From Experimental Measurements

Material	T (K)	σ_{xx}^{c} $\left(\frac{10^6}{\Omega\mathrm{m}}\right)$	$\sigma_{xy}^{s_z}$ $\left(\frac{\hbar}{e}\frac{10^3}{\Omega\mathrm{m}}\right)$	Θ_{SH} (%)	Ref.
Al	4.2	17	2.7 ± 6	$0.02\ \pm0.01$	[9]
Au	4.5	48.3	<1110	<2.3	[97]
	293	25.2	88 ± 8	$0.35\ \pm0.03$	[15]
	293	5.3	84 ± 5	$1.6\ \pm0.1$	[98]
	293	7.0	23.4 ± 0.4	0.335 ± 0.006	[98]
	293	20	50 ± 10	$0.25\ \pm0.05$	[99]
	295	37	≈ 4200	≈ 11	[100]
	295	25.7	<694	<2.7	[97]
Bi	3	0.0247	>0.198	>0.8	[101]
$Cu_{99.5}Bi_{0.5}$	10	8.8	≈ -970	$-11.0\ \pm4.0$	[19]
$Cu_{88}Ir_{12}$	10	2	≈ 43	$2.1\ \pm0.6$	[102]
Mo	10	2.8	-23 ± 5	$-0.8\ \pm0.18$	[16]
	293	4.66	-2.3 ± 0.5	$-0.05\ \pm0.0$	[15]
Nb	10	1.1	-10 ± 2	$-0.87\ \pm0.2$	[16]
Pd	10	2.2	27 ± 9	$1.2\ \pm0.4$	[16]
	293	4.0	26 ± 4	$0.64\ \pm0.1$	[15]
	293	1.97	≈ 20	≈ 1	[103]
	293	3.7	30 ± 7	$0.8\ \pm0.2$	[104]
	293	2.4	29 ± 5	$1.2\ \pm0.2$	[99]
Pt	10	8.1	170 ± 40	$2.1\ \pm0.5$	[16]
	293	6.4	≈ 510	≈ 8	[105]
	293	2.4	31 ± 5	$1.3\ \pm0.2$	[15]
	293	2.0	≈ 80	≈ 4	[106]
	293	5	340 ± 30	$6.8\ \pm0.5$	[107]
	293	2.42	97 ± 12	$4.0\ \pm0.5$	[108]
	293	4.3	51.6 ± 3	$1.2\ \pm0.2$	[109]
	293	3.6	76 ± 14	$2.2\ \pm0.4$	[104]
	293	1.02	20.51 ± 0.03	2.012 ± 0.003	[98]
	293	1.2	≈ 47	≈ 4	[110]
	293	2.45	74 ± 100	$3.\ \pm4.$	[111]
	293	4	110 ± 10	$2.7\ \pm0.3$	[99]
	300	3.05	330 ± 240	$11.\ \pm8.$	[112]
Ta	10	0.3	-1.1 ± 0.3	$-0.37\ \pm0.11$	[16]
	293	0.53	≈ -63	$-12.\ \pm4.$	[17]
	293	0.08	-1.6 ± 1.2	$-2.\ \pm1.5$	[111]
W	293	0.38	-127 ± 23	$-33.\ \pm6.$	[18]

[Hoffmann, IEEE Trans. Magn. 49 (2013) 5172]

4. Spintronics, magneto-devices and spin Hall effect

1) Spintronics (spin electronics)

Three basic elements: Generation, detection, & manipulation of spin current.

Usual spin current generations: Ferromagnetic leads

Problems: magnets and/or magnetic fields needed, and difficult to integrate with semiconductor technologies.

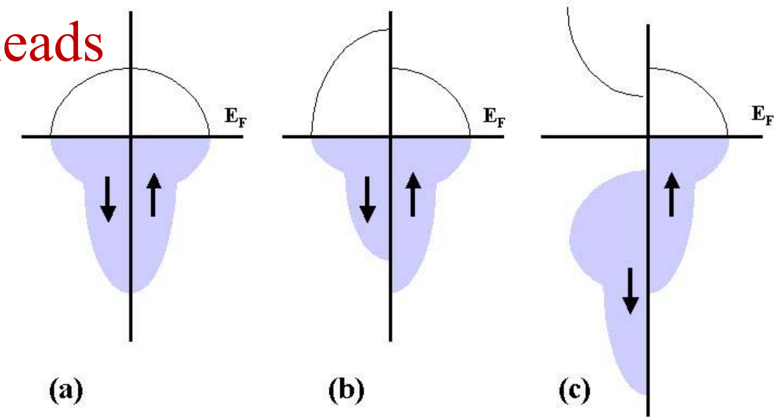

(a) non-magnetic metals, (b) ferromagnetic metals and (c) half-metallic metals.

(1) Direct spin Hall effect would allow us to generate pure spin current electrically in nonmagnetic microstructures without applied magnetic fields or magnetic materials, and make possible pure electric driven spintronics which could be readily integated with conventional electronics.

(2) Inverse spin Hall effect would enable us to detect spin current electrically, again without applied magnetic fields or magnetic materials.

2) Magneto-electric devices

Spin-torque switching with the giant spin Hall effect of tantalum

[Liu et al., Science 336, 555 (2012)]

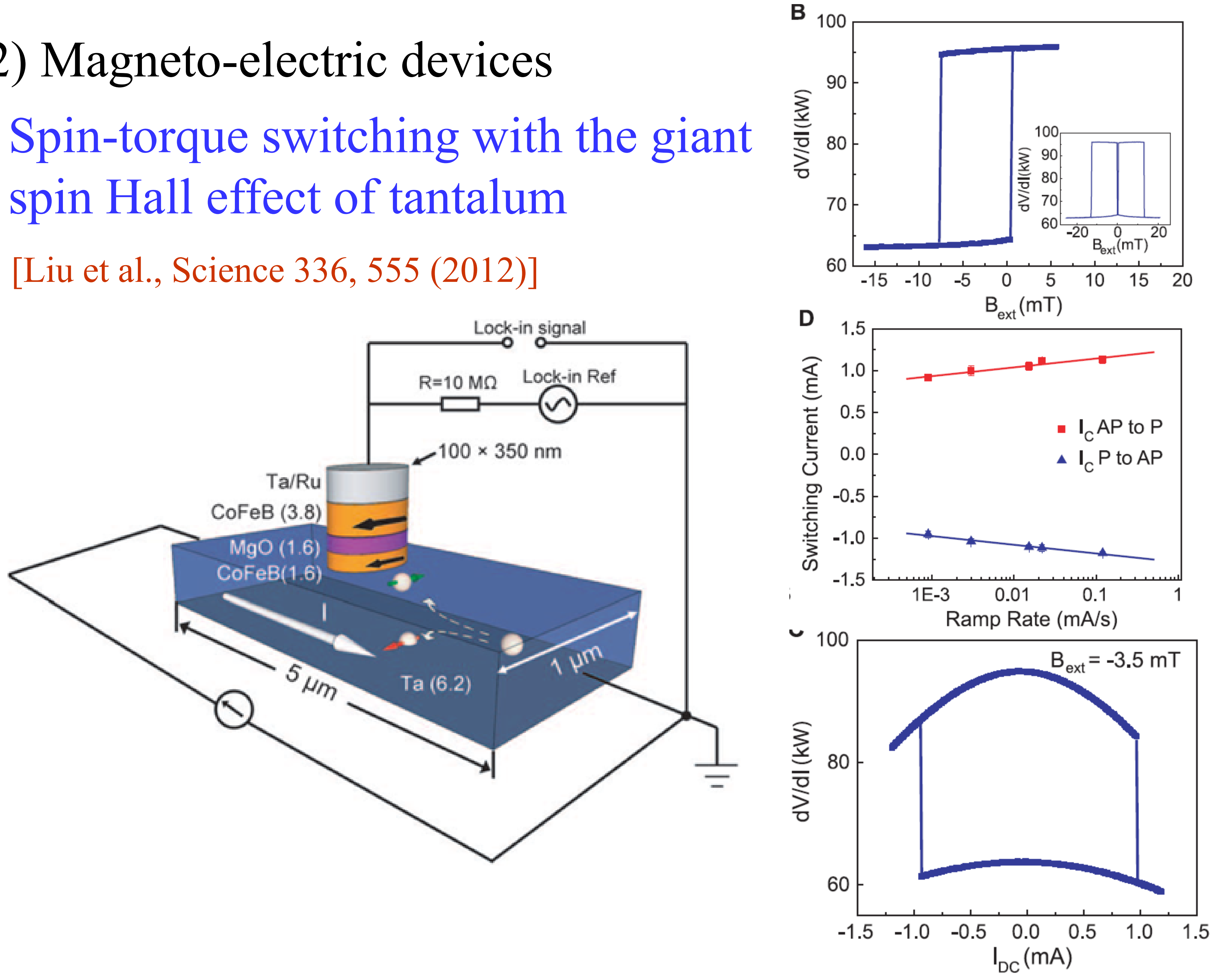

5. Spin-off's: Topological insulators and spin caloritronics

Quantum Hall effect in conventional 2DEG

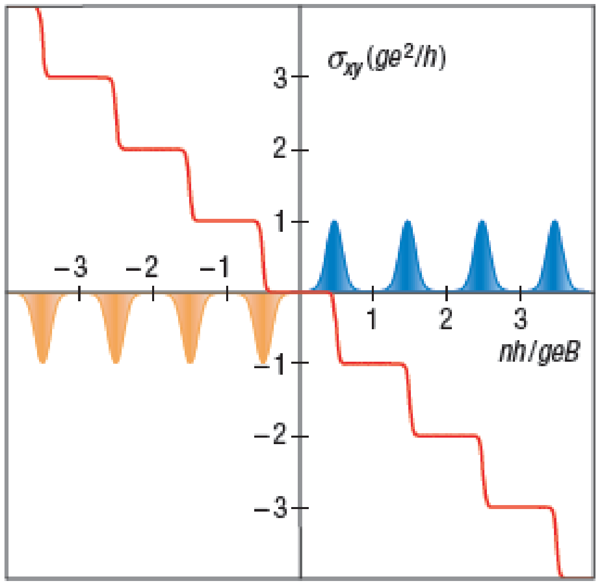

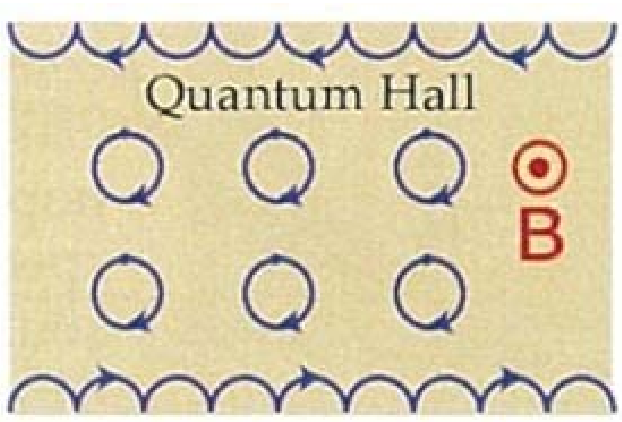

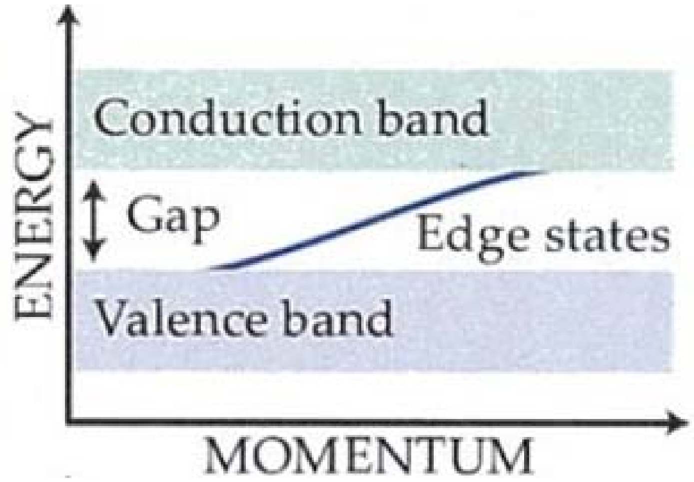

[Laughlin, PRB23, 5632 (1981)]

$$\sigma_{xy} = \pm \nu \frac{2e^2}{h}, \nu = \text{Chern (TKNN) number}$$

$$\nu = \frac{1}{2\pi} \sum_n \int_{\mathrm{BZ}} dk_x dk_x \Omega^n_{xy}(\mathbf{k})$$

[Thouless et al., PRL49, 405 (1982)]

Quantum Hall states are insulating with broken time-reversal symmetry.
Topological invariant is Chern number.

2D Topological insulators from quest for quantum spin Hall effect

[Kane & Mele, PRL 95 (2005) 146801]

Kane-Mele SOC Hamiltonian for graphene

$$H_{\mathrm{KM}} = t\sum_{<i,j>} c_i^{\dagger} c_j + i\lambda \sum_{<<ij>>} c_i^{\dagger} s_z v_{ij} c_j$$

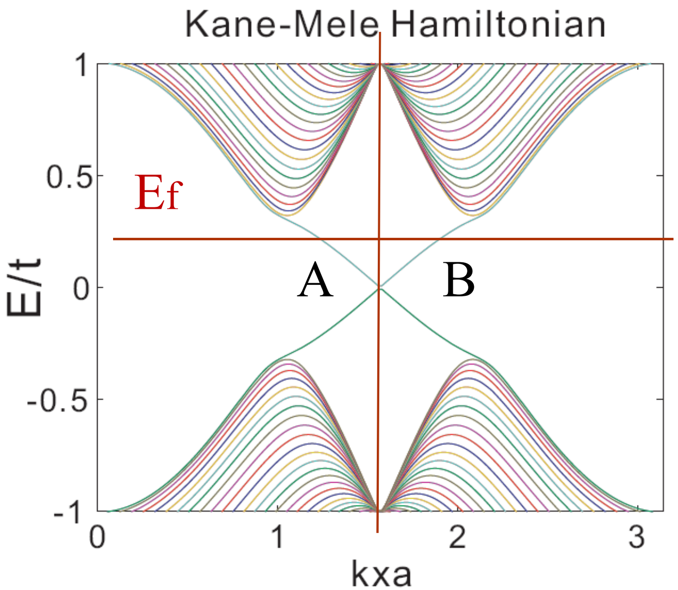

$$\sigma_{xy}^{s} = |\nu|\frac{e}{2\pi},\ \ \sigma_{xy} = 0.$$

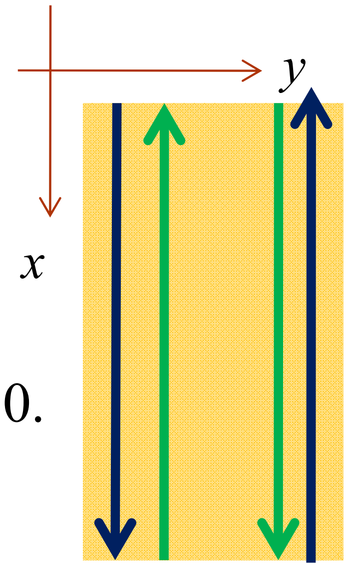

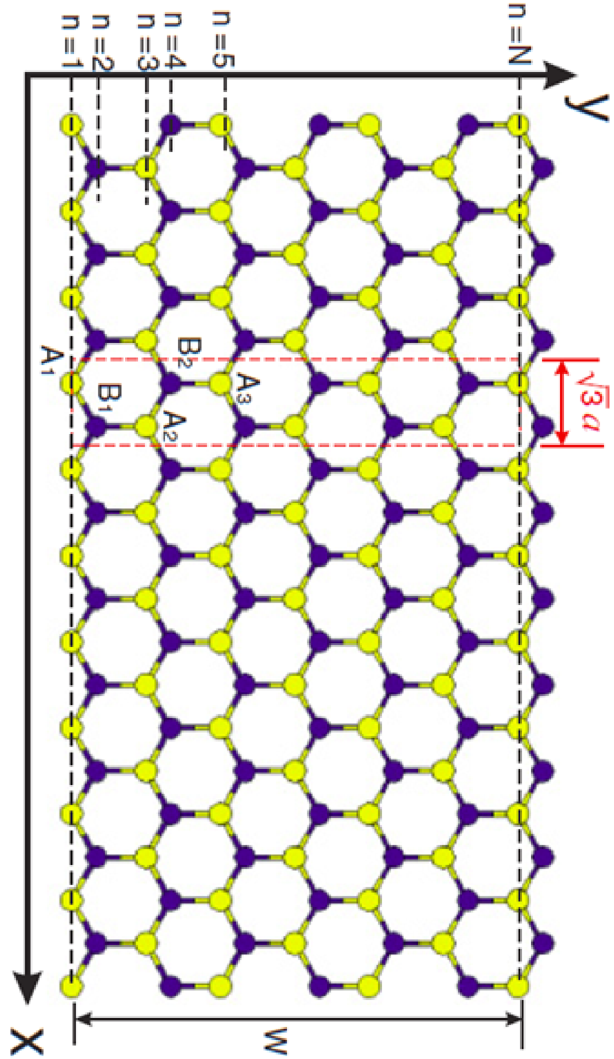

no SOC

SOC

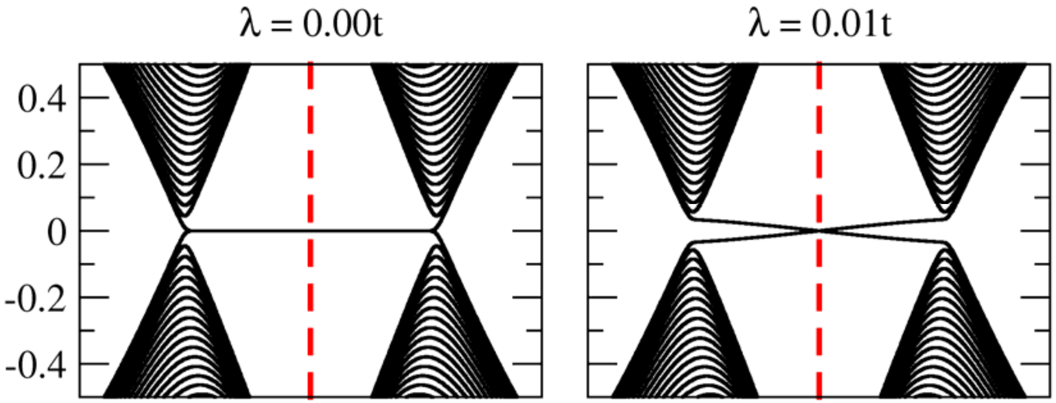

SOC is too small (<0.01 meV) to make QSHE observable!

[Chen, Xiao, Chiou, Guo, PRB 84, 165453 (2011)]

Quantum spin Hall effect in topological phase in HgTe quantum well

[Bernevig, Hughes, Zhang, Science 314, 1757 (2006)]

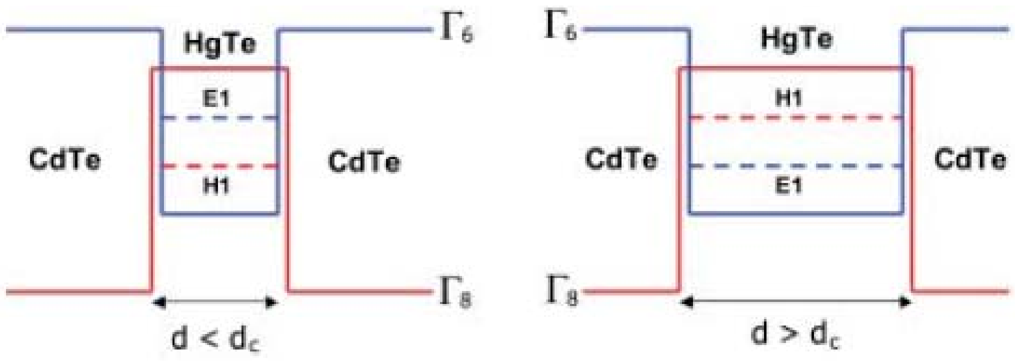

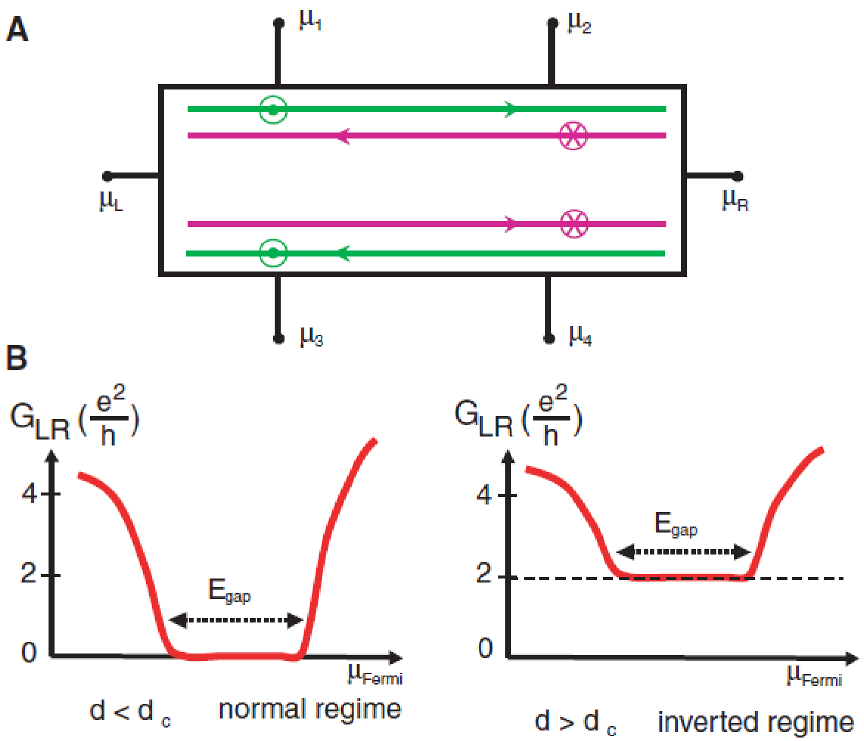

Evidence for quantum spin Hall effect in quantum wells

[Koenig et al., Science 318, 766 (2007)]

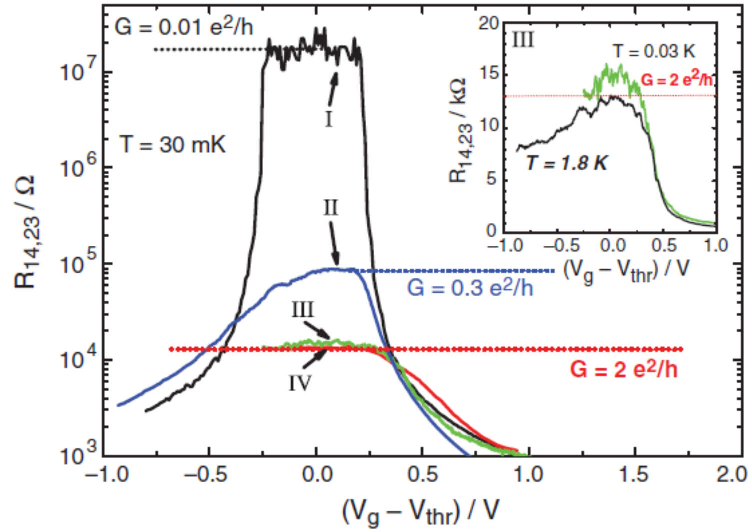

[Du et al., arXiv.1306.1925]

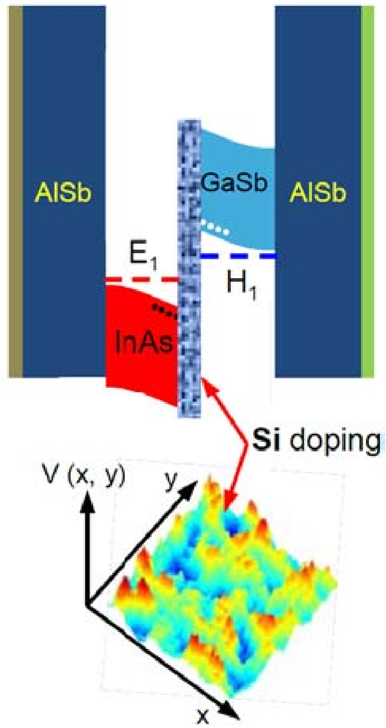

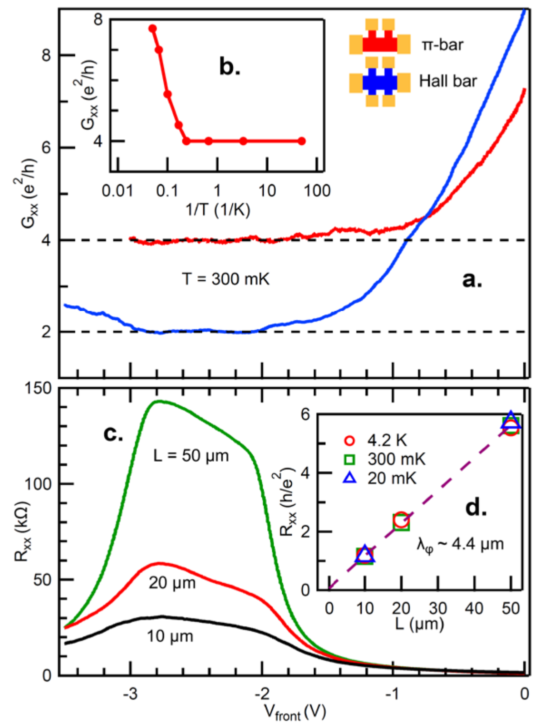

3D Topological insulators

[Fu, Kane, Mele, PRL98, 106803(the.)]

Host a number of exotic phenemona, e.g., majorana fermion superconductivity, axion electrodynamics and quantum anomalous Hall effect

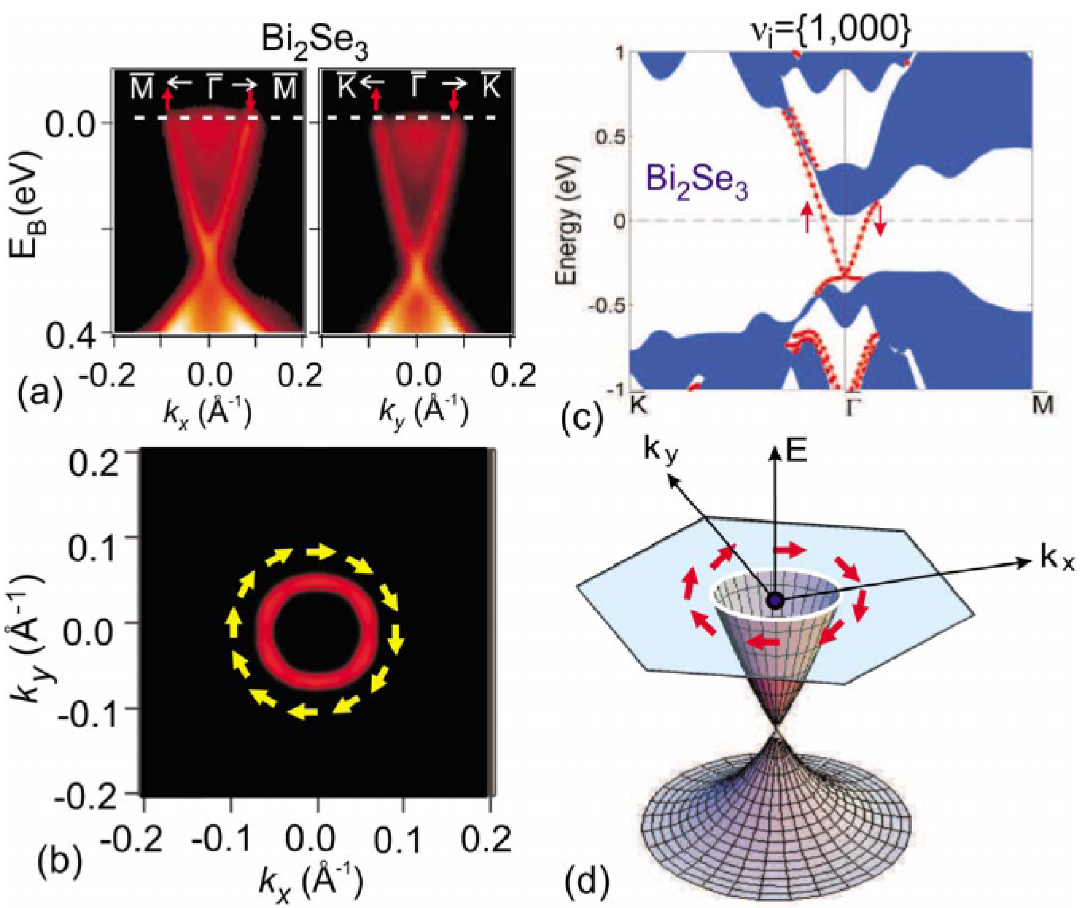

[Hsieh et al., Nature 460 (2009) 1101;
Xia et al., NP 5 (2009) 398]

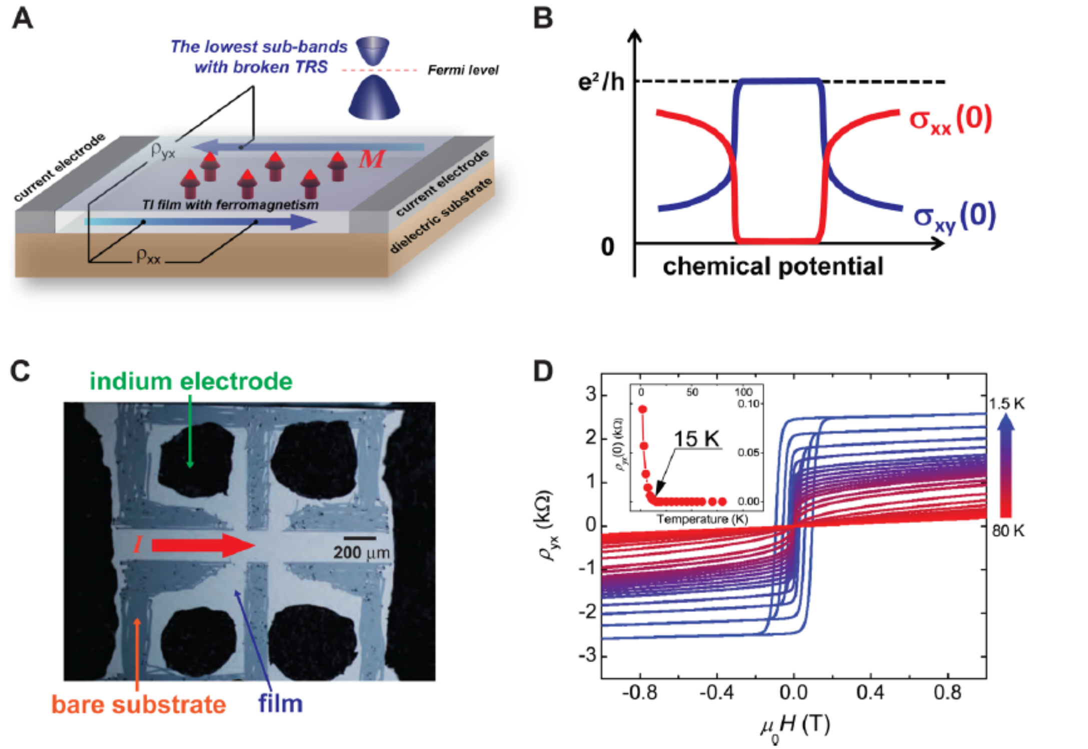

observed in $Cr_{0.15}(Bi_{0.1}Sb_{0.9})_{1.85}Te_3$ film

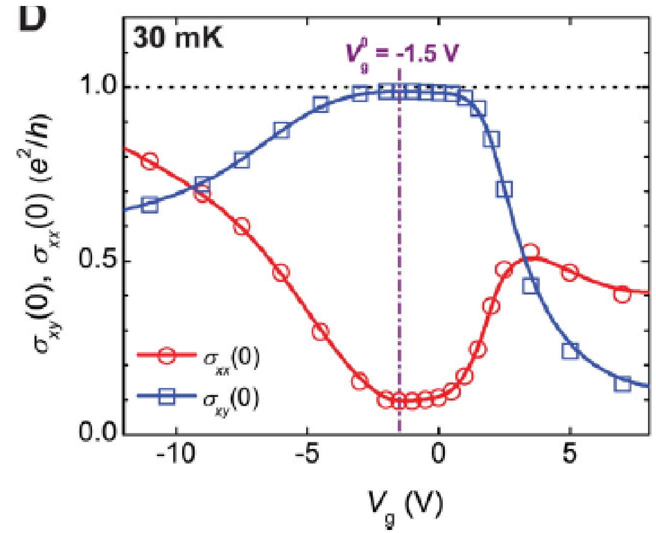

[Chang et al. Science 340, 167 (2013)]

2. Spin caloritronics

[Bauer, Saitoh, van Wees, Nature Mater. 11 (2012) 391]

Spin Nernst effect

Spin Hall Effect

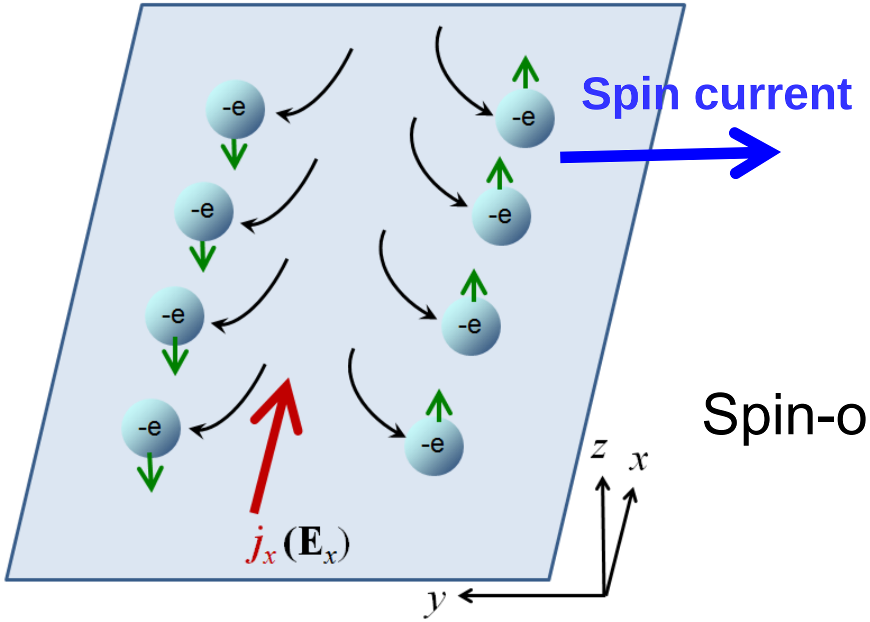

Spin-orbit interactioı

$$\frac{dV(r)}{dr}(\mathbf{s}\cdot\mathbf{L})$$

Spin Nernst Effect

[Cheng et al., PRB 2008]

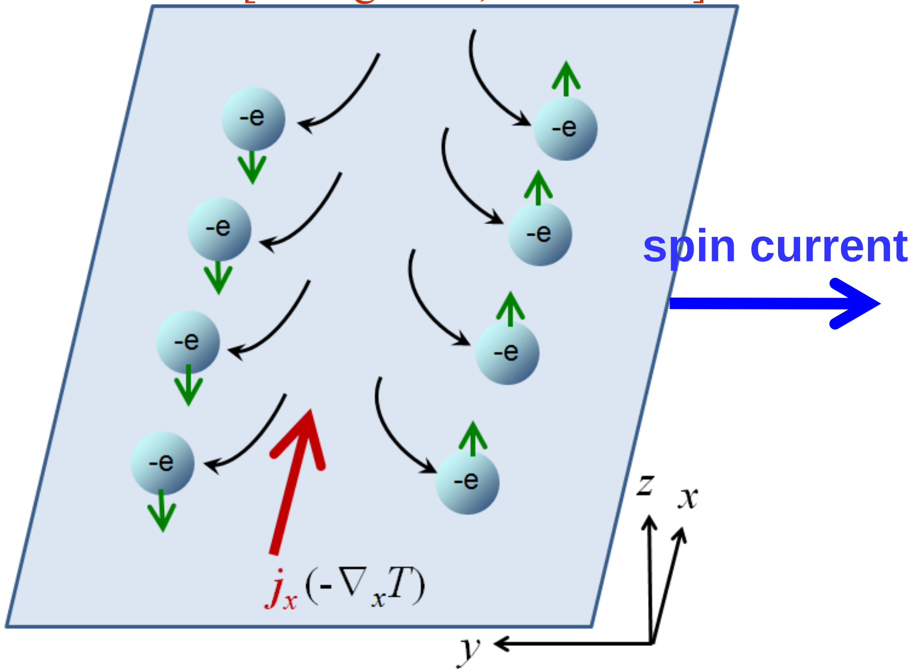

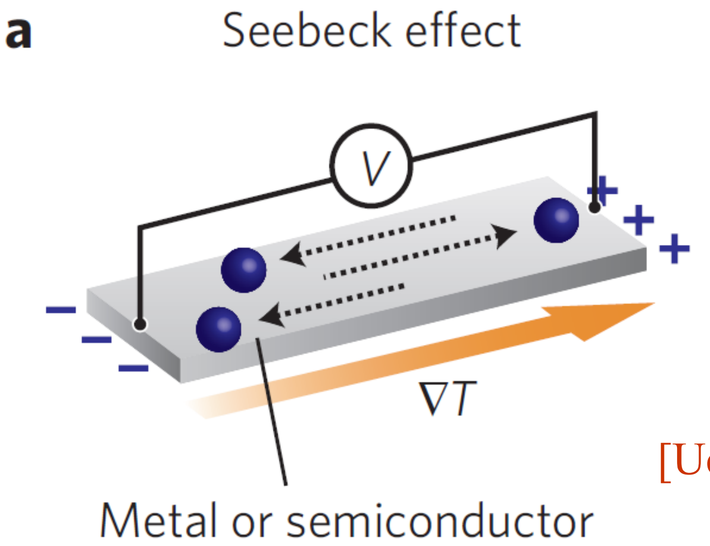

Spin Seebeck effect

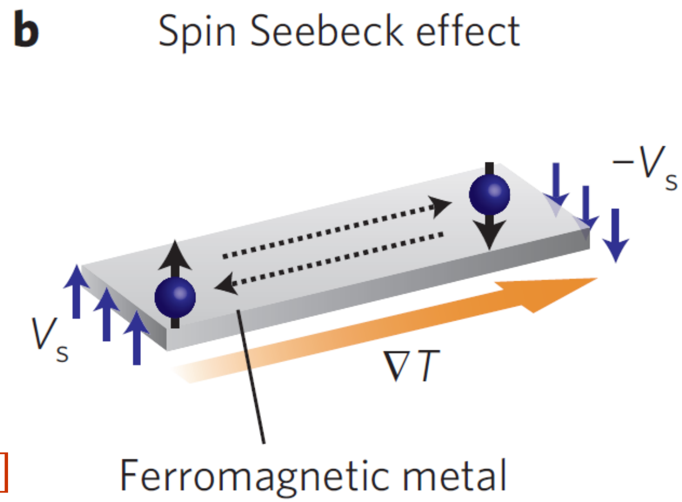

[Uchida et al., Nature 455 (2008) 778]

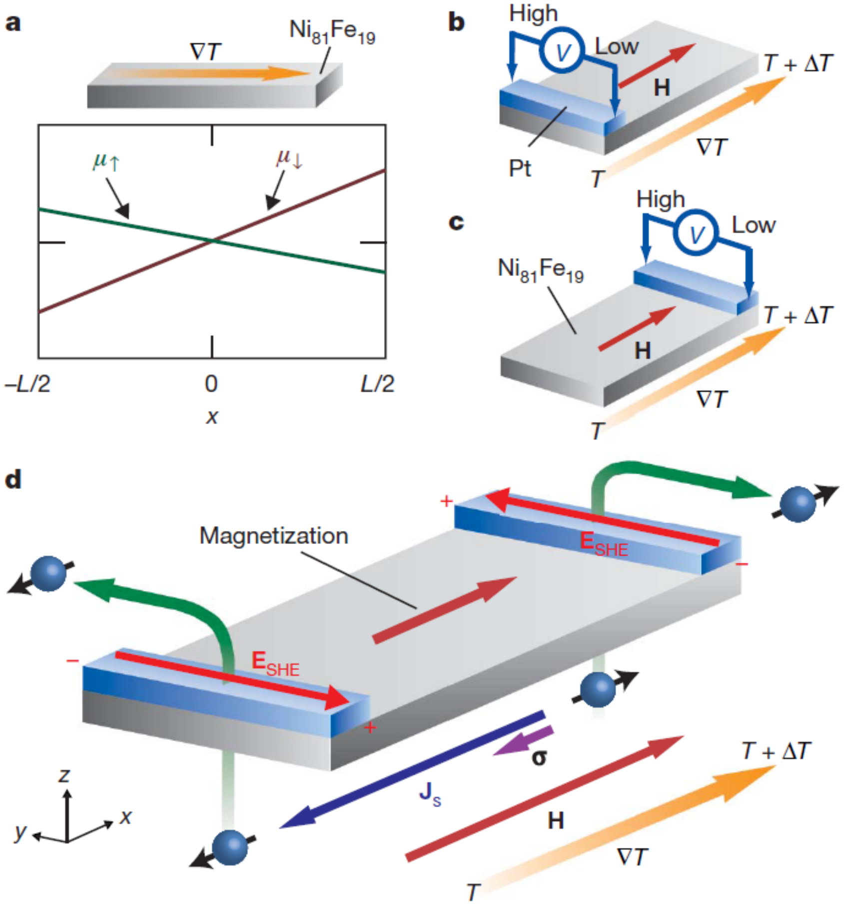

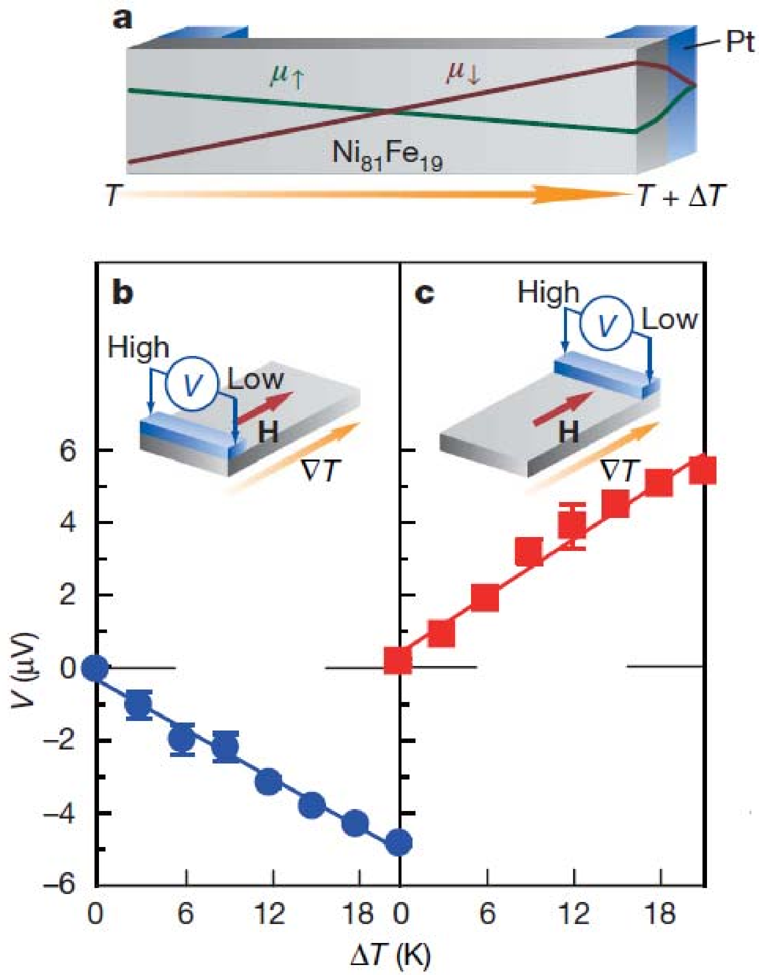

Thus, we could have thermally driven spintronic devices, i.e., spin caloritronics.

II. *Ab initio* studies of intrinsic spin Hall effect in solids

1. Motivations

1) Will the intrinsic spin Hall effect exactly cancelled by the intrinsic orbital-angular-momentum Hall effect?

[S. Zhang and Z. Yang, cond-mat/0407704; PRL 2005]

In conclusion, we have shown that the ISHE is accompanied by the intrinsic orbital-angular-momentum Hall effect so that the total angular momenttum spin current is zero in a SOC system.

For Rashba Hamiltonian, $\mathcal{J}_{int}^{spin} = \frac{e}{8\pi}E; \quad J_{int}^{orbit} = -\frac{e}{8\pi}E.$

This is confirmed for Rashba system by us. However, in Dresselhaus and Rashba systems, spin Hall conductivity would not be cancelled by the orbital Hall conductivity.

[Chen, Huang, Guo, PRB73 (2006) 235309]

2) To go beyond the spherical 4-band Luttinger Hamiltonian.

3) To understand the effects of epitaxial strains.

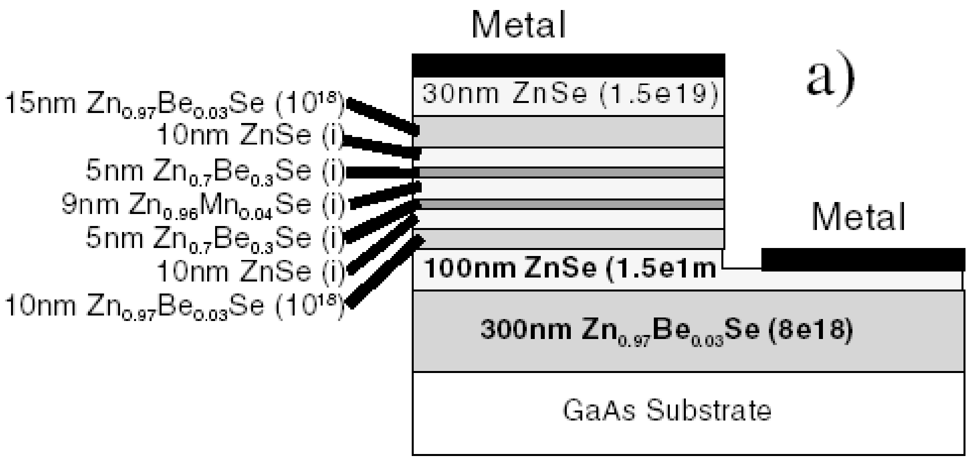

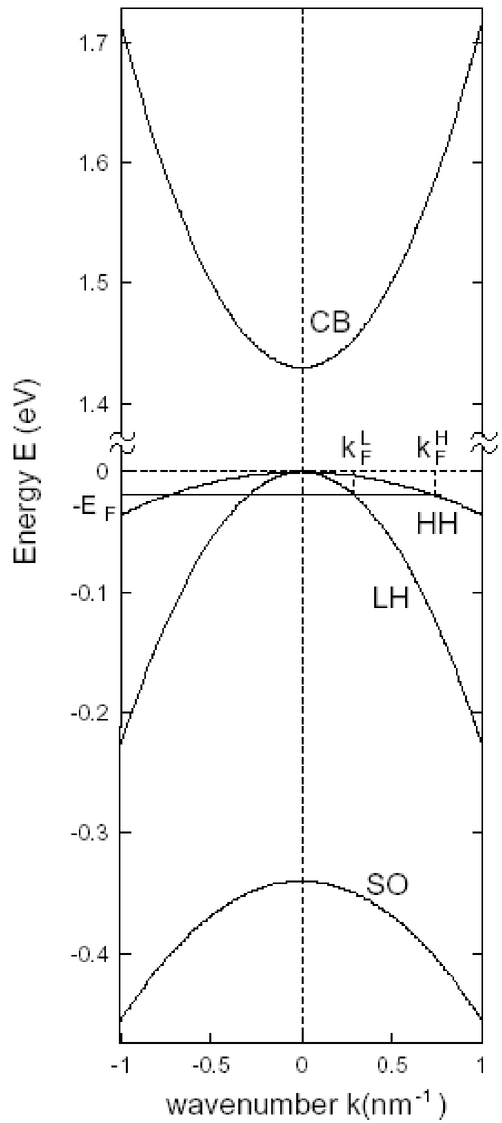

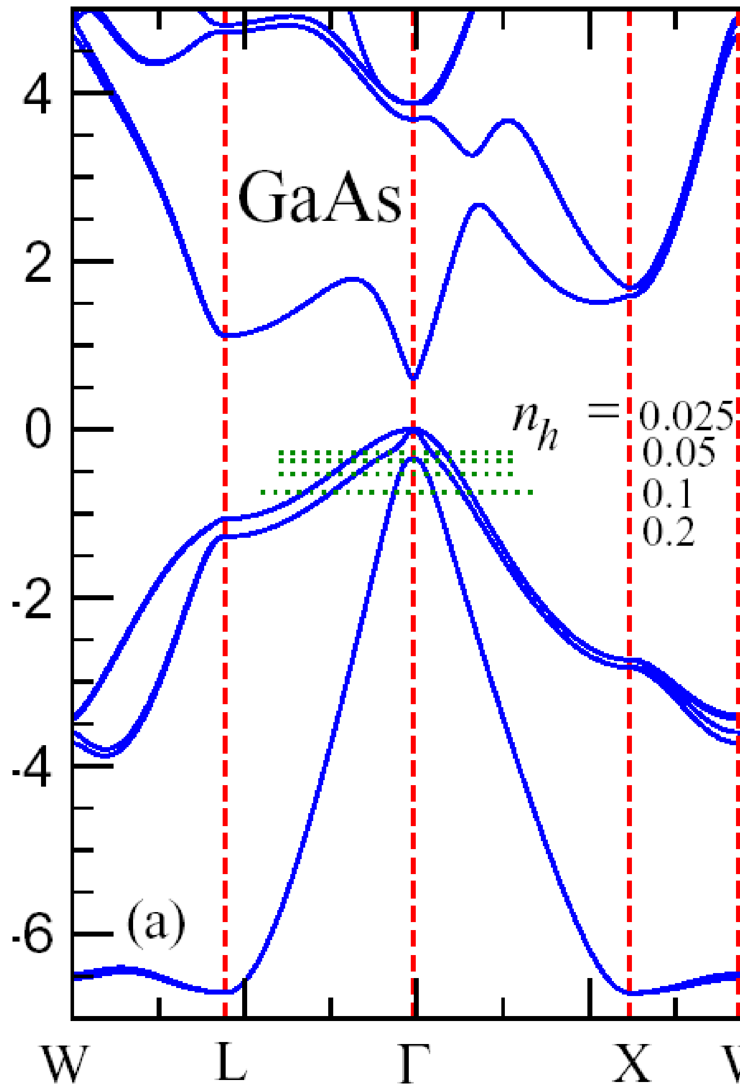

4) To understand the detailed mechanism of the SHE in metals because it would lead to the material design of the large SHE even at room temperature with the application to the spintronics. To this end, *ab initio* band theoretical calculations for real metal systems is essential.

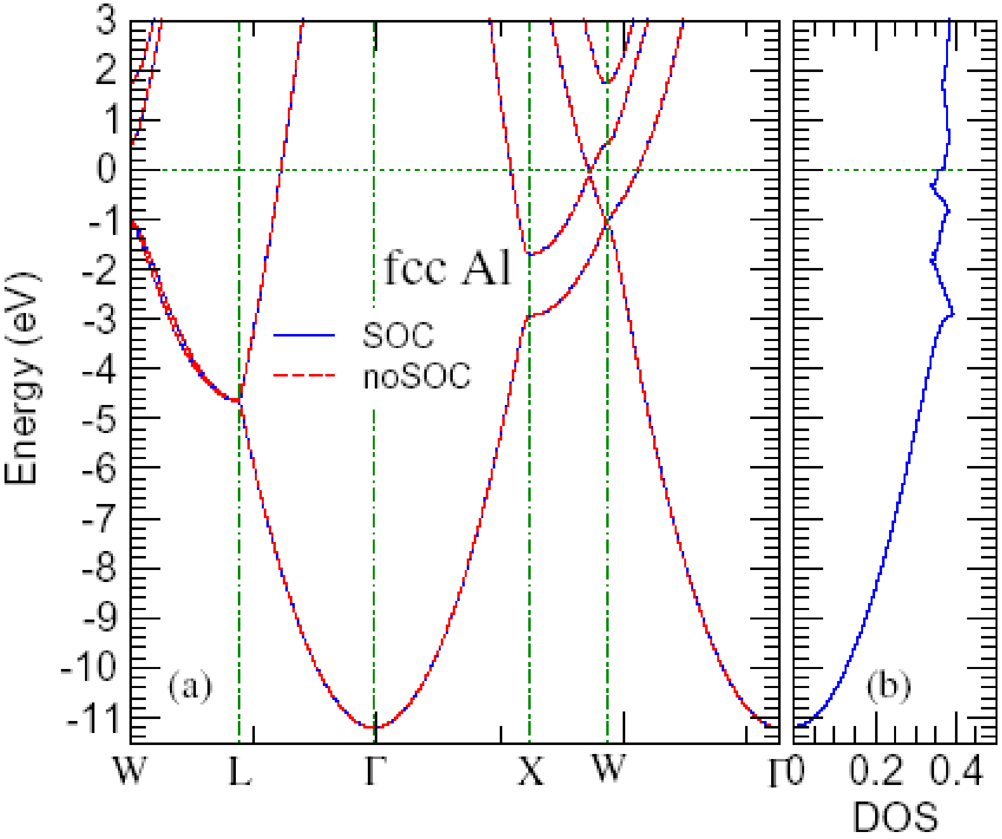

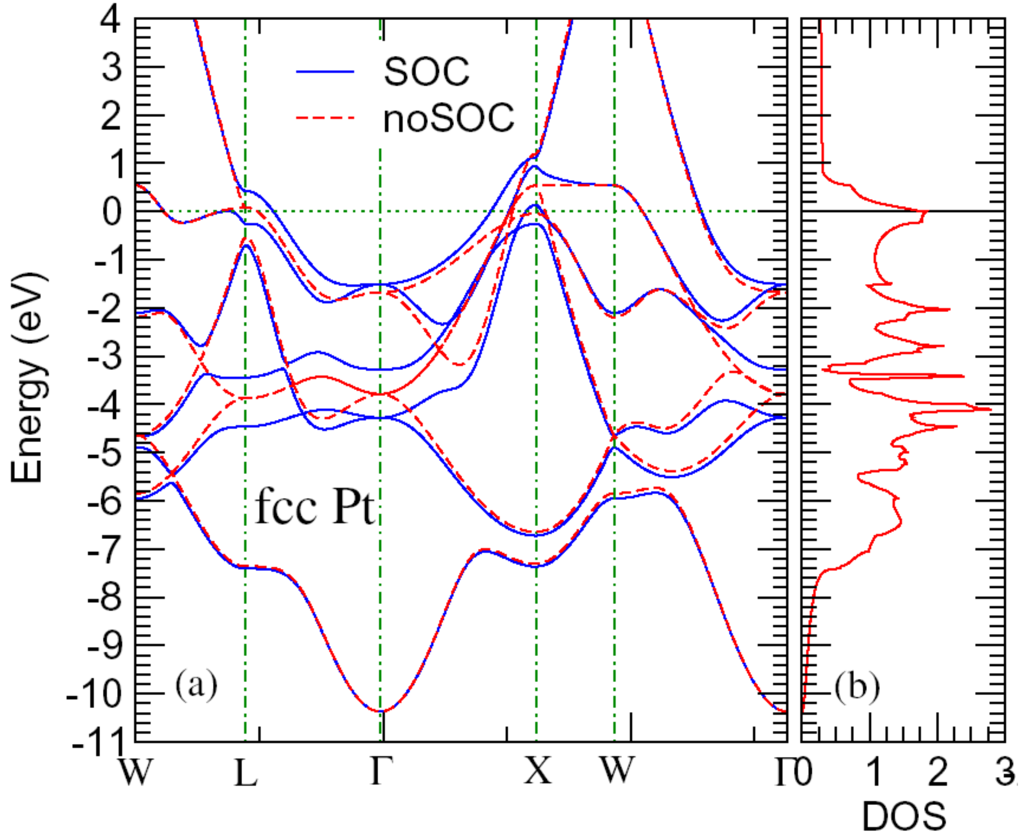

2. Berry phase formalism for intrinsic Hall effects

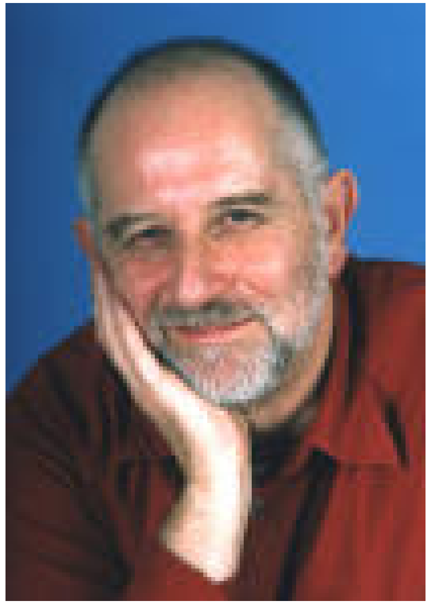

1) Berry phase

[Berry, Proc. Roy. Soc. London A 392, 451 (1984)]

Parameter dependent system:

$$\{\,\varepsilon_n(\lambda),\ \psi_n(\lambda)\,\}$$

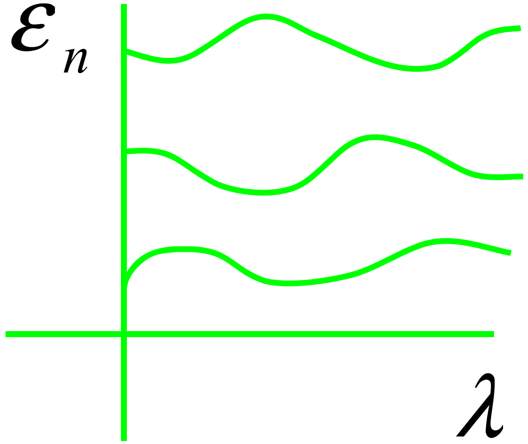

Adiabatic theorem:

$$\Psi(t) = \psi_n(\lambda(t))\ e^{-i\int_0^t dt\,\varepsilon_n/\hbar}\ e^{-i\gamma_n(t)}$$

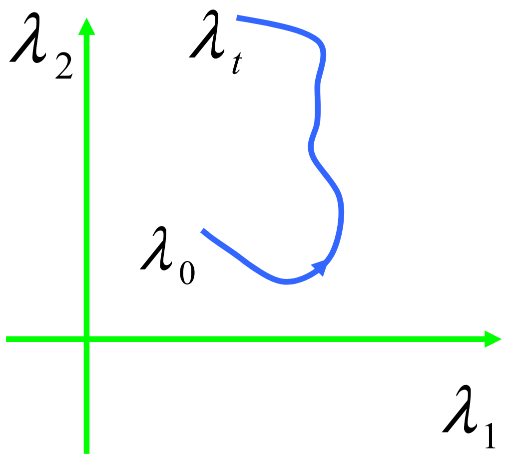

Geometric phase:

$$\gamma_n = \int_{\lambda_0}^{\lambda_t} d\lambda\,\langle \psi_n | i\frac{\partial}{\partial\lambda} | \psi_n \rangle$$

Well defined for a closed path

$$\gamma_n = \oint_C d\lambda \left\langle \psi_n \middle| i \frac{\partial}{\partial \lambda} \middle| \psi_n \right\rangle$$

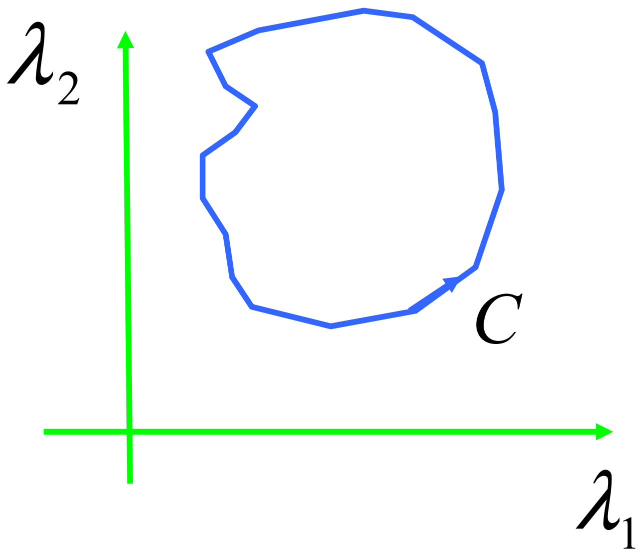

Stokes theorem

$$\gamma_n = \iint d\lambda_1 d\lambda_2 \, \Omega$$

Berry Curvature

$$\Omega = i \frac{\partial}{\partial \lambda_1} \left\langle \psi \middle| \frac{\partial}{\partial \lambda_2} \middle| \psi \right\rangle - i \frac{\partial}{\partial \lambda_2} \left\langle \psi \middle| \frac{\partial}{\partial \lambda_1} \middle| \psi \right\rangle$$

Analogies

Berry curvature

$$\Omega(\vec{\lambda})$$

Berry connection

$$\langle \psi | i \frac{\partial}{\partial \lambda} | \psi \rangle$$

Geometric phase

$$\oint d\lambda \langle \psi | i \frac{\partial}{\partial \lambda} | \psi \rangle = \iint d^2\lambda \;\; \Omega(\vec{\lambda})$$

Chern number

$$\oiint d^2\lambda \;\; \Omega(\vec{\lambda}) = \text{integer}$$

Magnetic field

$$B(\vec{r})$$

Vector potential

$$A(\vec{r})$$

Aharonov-Bohm phase

$$\oint dr \; A(\vec{r}) = \iint d^2 r \; B(\vec{r})$$

Dirac monopole

$$\oiint d^2 r \;\; B(\vec{r}) = \text{integer } h/e$$

2) Semiclassical dynamics of Bloch electrons

Old version [e.g., Aschroft, Mermin, 1976]

$$\dot{\mathbf{x}}_c = \frac{1}{\hbar}\frac{\partial \varepsilon_n(\mathbf{k})}{\partial \mathbf{k}},$$

$$\dot{\mathbf{k}} = -\frac{e}{\hbar}\mathbf{E} - \frac{e}{\hbar}\dot{\mathbf{x}}_c \times \mathbf{B} = \frac{e}{\hbar}\frac{\partial \varphi(\mathbf{r})}{\partial \mathbf{r}} - \frac{e}{\hbar}\dot{\mathbf{x}}_c \times \mathbf{B}.$$

New version [Marder, 2000]

Berry phase correction [Chang & Niu, PRL (1995), PRB (1996)]

$$\dot{\mathbf{x}}_c = \frac{1}{\hbar}\frac{\partial \varepsilon_n(\mathbf{k})}{\partial \mathbf{k}} - \dot{\mathbf{k}} \times \mathbf{\Omega}_n(\mathbf{k}),$$

$$\dot{\mathbf{k}} = \frac{e}{\hbar}\frac{\partial \varphi(\mathbf{r})}{\partial \mathbf{r}} - \frac{e}{\hbar}\dot{\mathbf{x}}_c \times \mathbf{B},$$

$$\mathbf{\Omega}_n(\mathbf{k}) = -\,\mathrm{Im}\left\langle \frac{\partial u_{n\mathbf{k}}}{\partial \mathbf{k}} \right| \times \left| \frac{\partial u_{n\mathbf{k}}}{\partial \mathbf{k}} \right\rangle. \quad \text{(Berry curvature)}$$

3) Semiclassical transport theory

$$\mathbf{j} = \int d^3k(-e\dot{\mathbf{x}})g(\mathbf{r},\mathbf{k}), \qquad g(\mathbf{r},\mathbf{k}) = f(\mathbf{k}) + \delta f(\mathbf{r},\mathbf{k})$$

$$\dot{\mathbf{x}} = \frac{\partial \varepsilon_n(\mathbf{k})}{\hbar \partial \mathbf{k}} + \frac{e}{\hbar}\mathbf{E}\times\mathbf{\Omega}$$

(ordinary conductance)

$$\mathbf{j} = -\frac{e^2}{\hbar}\mathbf{E}\times\int d^3\mathbf{k} f(\mathbf{k})\mathbf{\Omega} - \frac{e}{\hbar}\int d^3\mathbf{k}\,\delta f(\mathbf{k},\mathbf{r})\frac{\partial \varepsilon_n(\mathbf{k})}{\partial \mathbf{k}}$$

(Anomalous Hall conductance)

Anomalous Hall conductivity

$$\sigma_{xy} = -\frac{e^2}{\hbar}\int d^3\mathbf{k}\sum_n f(\varepsilon_n(\mathbf{k}))\Omega_n^z(\mathbf{k})$$

$$\Omega_n^z(\mathbf{k}) = -\sum_{n'\neq n}\frac{2\,\mathrm{Im}\langle \mathbf{k}n|v_x|\mathbf{k}n'\rangle\langle \mathbf{k}n'|v_y|\mathbf{k}n\rangle}{(\omega_{\mathbf{k}n'}-\omega_{\mathbf{k}n})^2}$$

[FLAPW (WIEN2k) calculations]

σ_{xy} (S/cm)	theory	Exp.
bcc Fe	750[a]	1030
hcp Co	477[b]	480
fcc Ni	-1066[c]	-1100

[a][Yao, et al., PRL 92 (2004) 037204]
[b][Wang, et al., PRB 76 (2007) 195109]
[c][Fuh, Guo, PRB 84 (2011) 144427]

4) *Ab initio* relativistic band structure methods

Calculations must be based on a relativistic band theory because all the intrinsic Hall effects are caused by spin-orbit coupling.

Relativistic extension of linear muffin-tin orbital (LMTO) method.
[Ebert, PRB 1988; Guo & Ebert, PRB 51, 12633 (1995)]

Dirac Hamiltonian $H_D = c\boldsymbol{\alpha}\cdot\mathbf{p} + mc^2(\beta - I) + v(\mathbf{r})I$

$$\sigma_{xy} = \frac{e}{\hbar}\int d^3\mathbf{k}\sum_n f(\varepsilon_n(\mathbf{k}))\Omega_n^z(\mathbf{k})$$

$$\Omega_n^z(\mathbf{k}) = -\sum_{n'\neq n}\frac{2\,\mathrm{Im}\langle\mathbf{k}n|j_x|\mathbf{k}n'\rangle\langle\mathbf{k}n'|v_y|\mathbf{k}n\rangle}{(\omega_{\mathbf{k}n}-\omega_{\mathbf{k}n'})^2}$$

current operator $\mathbf{j} = -ec\alpha$ (AHE), (charge current operator)

$$\mathbf{j} = \frac{\hbar}{4}\{\beta\Sigma_z, c\alpha_i\}$$ (SHE), (spin current operator)

$$\mathbf{j} = \frac{\hbar}{2}\{\beta L_z, c\alpha\}$$ (OHE). (orbital current operator)

α, β, Σ are 4×4 Dirac matrices.

5) Application to intrinsic spin Hall effect in semiconductors

[Guo,Yao,Niu, PRL 94, 226601 (2005)]

Spin and orbital angular momentum Hall effects in p-type zincblende semicoductors

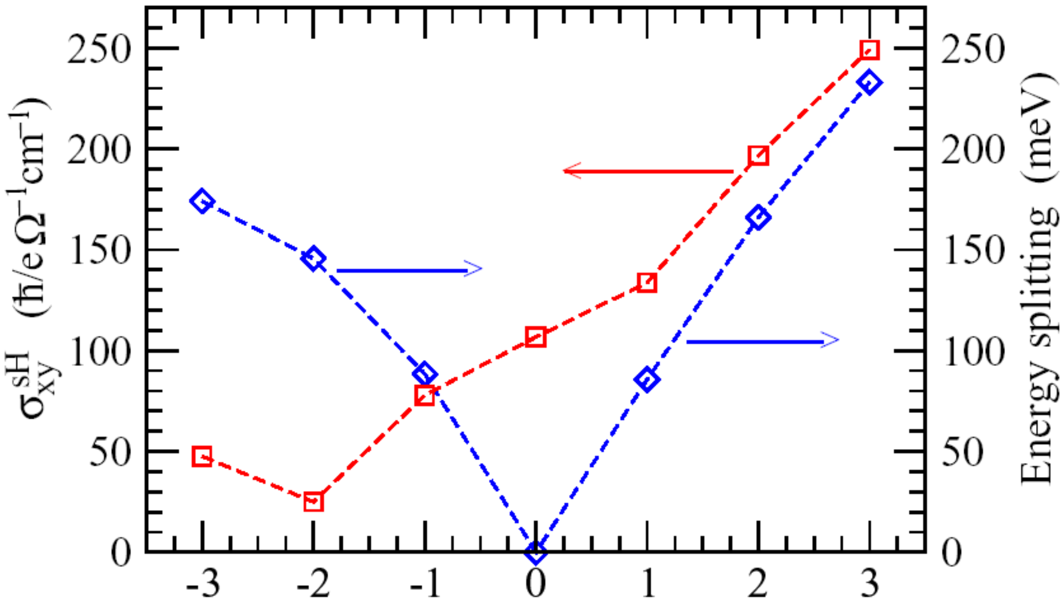

Strain effect

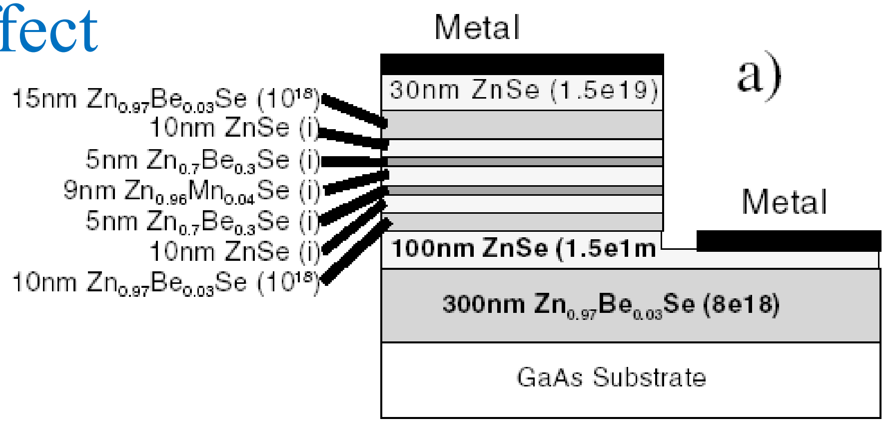

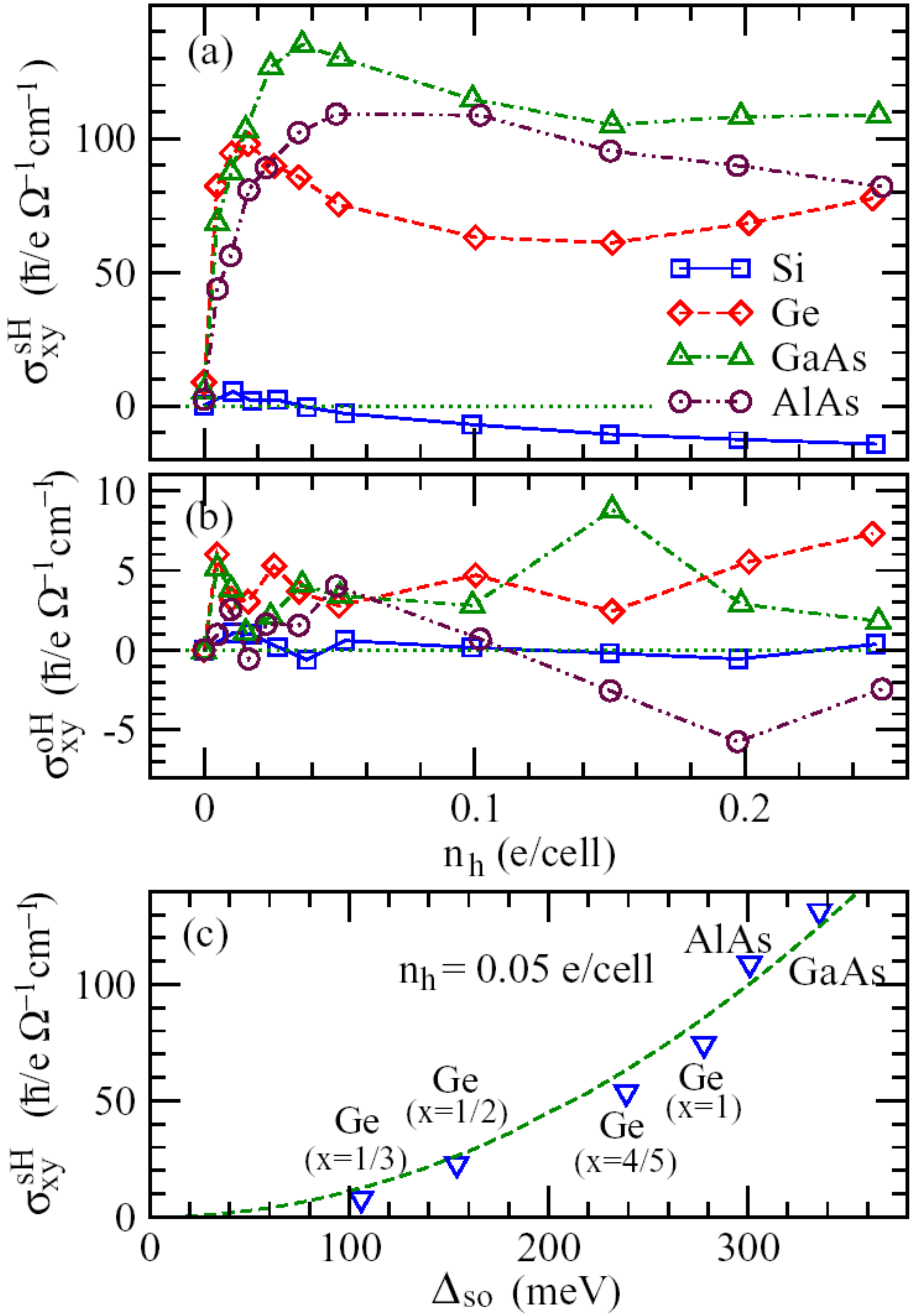

3. Large intrinsic spin Hall effect in platinum

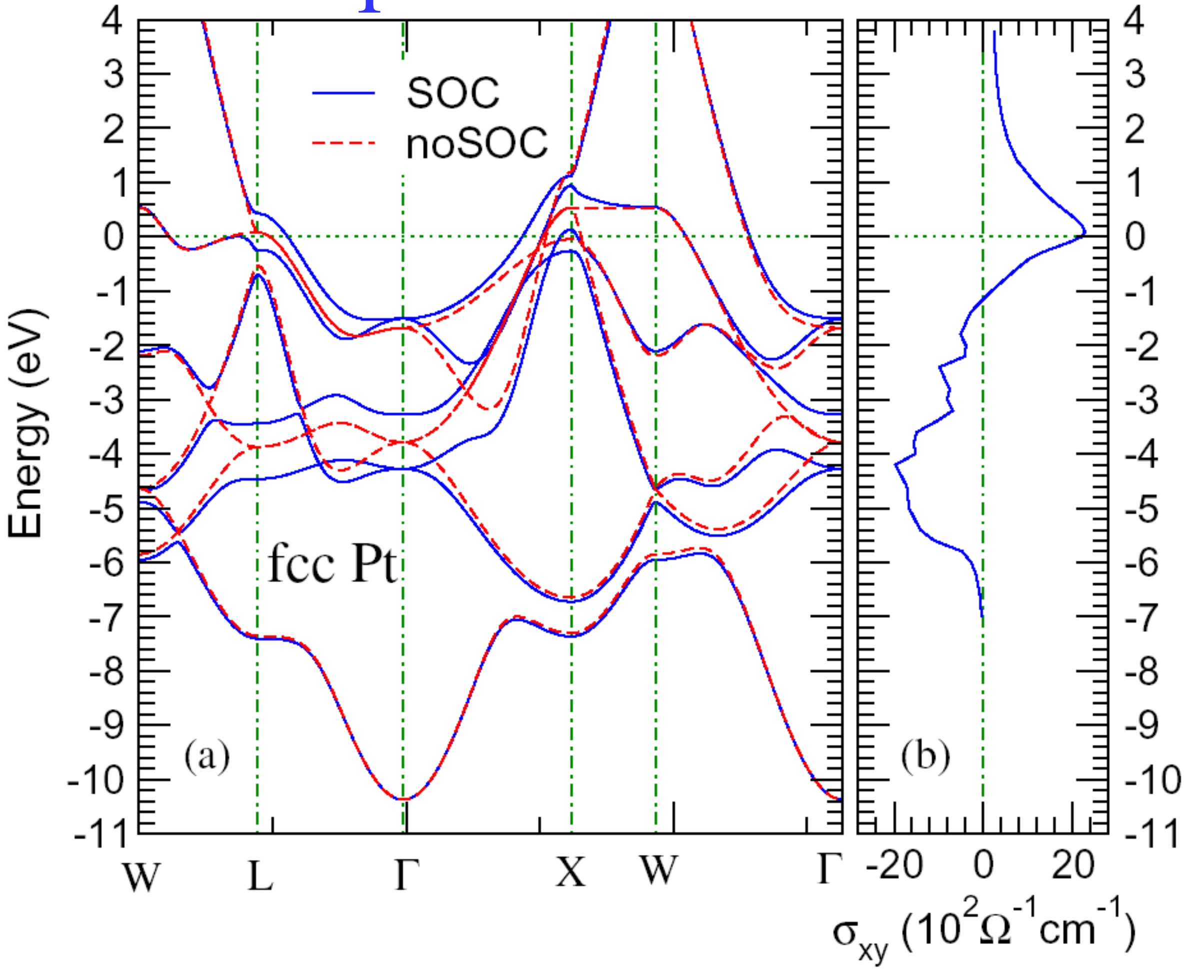

Al: σ_{sH} (4.2 K) = 17 $(\Omega cm)^{-1}$

σ_{sH} (exp., 4.2K) = 27, 34 $(\Omega cm)^{-1}$

[Valenzuela, Tinkham, Nature 442, 176 (2006)]

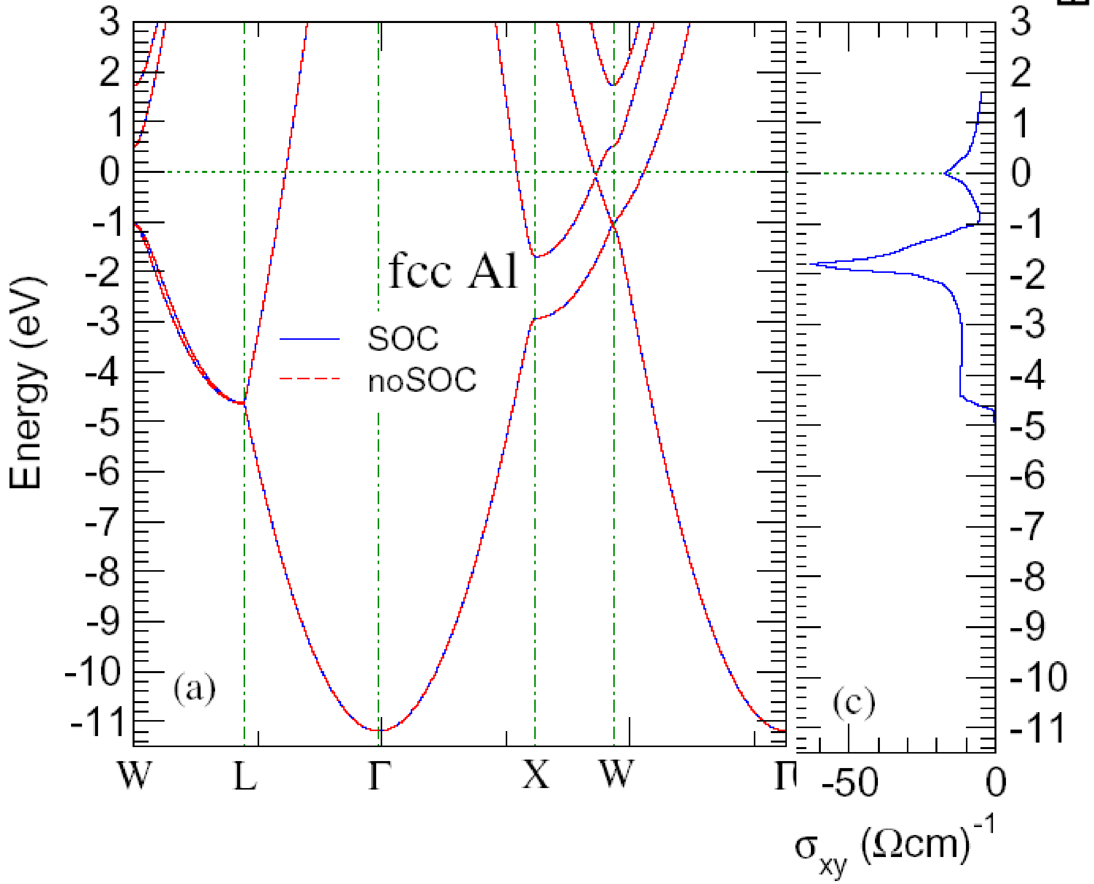

Pt: σ_{sH} = 2200 $(\Omega cm)^{-1}$ (T = 0 K)

[Guo, Murakami, Chen, Nagaosa, PRL100, 096401 (2008)]

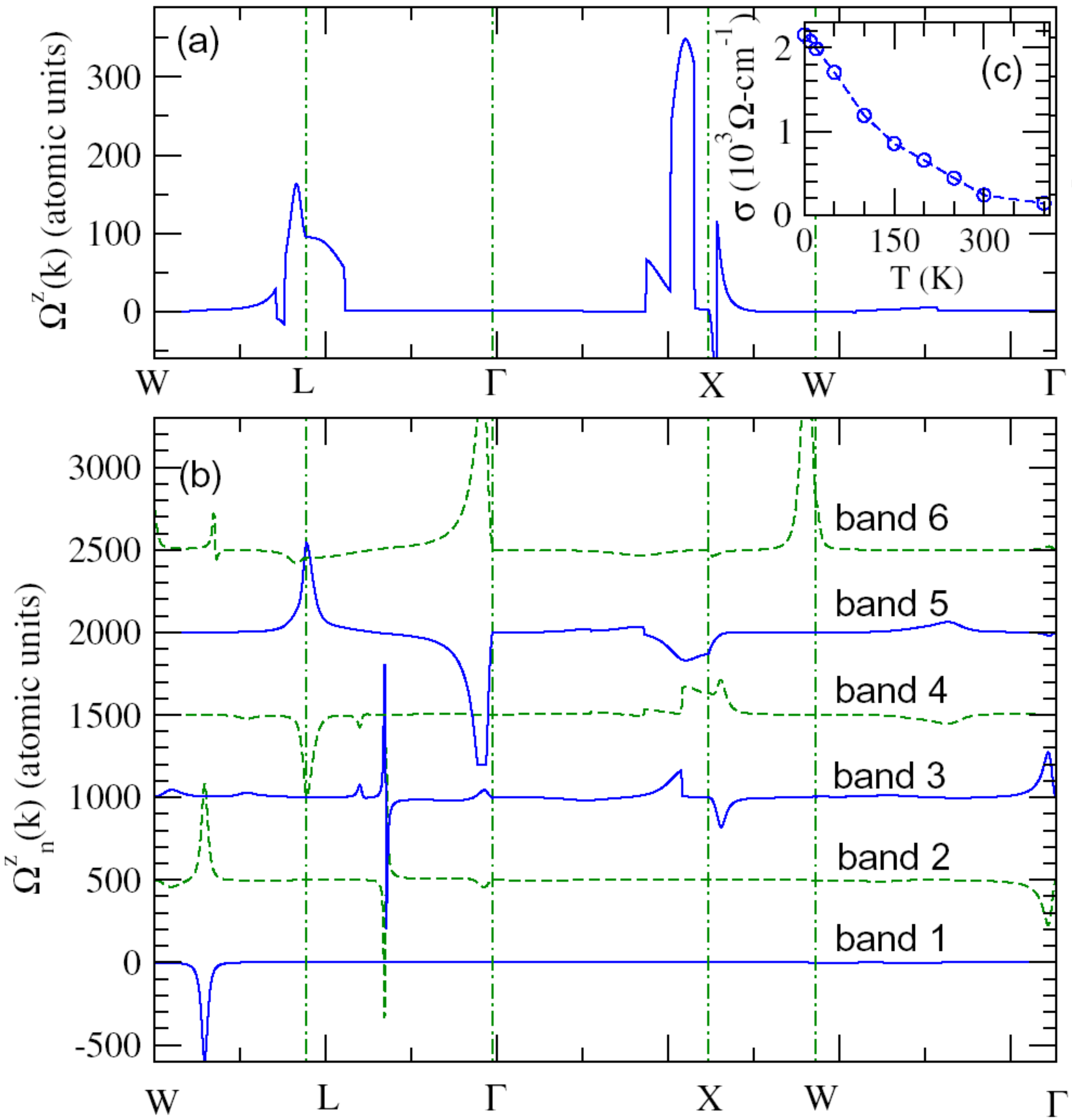

$$\sigma_{xy} = -\frac{e}{\hbar}\sum_{\mathbf{k}} \Omega^z(\mathbf{k}) = \frac{e}{\hbar}\sum_{\mathbf{k}}\sum_{n} f(\varepsilon_n(\mathbf{k}))\Omega^z_n(\mathbf{k})$$

$$\Omega^z_n(\mathbf{k}) = \sum_{n'\neq n} \frac{2\,\mathrm{Im}\langle \mathbf{k}n \mid j^z_x \mid \mathbf{k}n'\rangle\langle \mathbf{k}n' \mid v_y \mid \mathbf{k}n\rangle}{(\omega_{\mathbf{k}n} - \omega_{\mathbf{k}n'})^2}$$

Pt: σ_{sH} (300K) = 240 $(\Omega\mathrm{cm})^{-1}$

σ_{sH} (exp., RT) = 240 $(\Omega\mathrm{cm})^{-1}$

[Kimura et al PRL98, 156601 (2007)]

Pt: σ_{sH} (0K) = 2200 $(\Omega\mathrm{cm})^{-1}$

σ_{sH} (exp., 5 K) = 1700 $(\Omega\mathrm{cm})^{-1}$

[Morota et al, PRB83, 174405 (2011)]
[Hoffmann,
IEEE Trans. Magn. 49 (2013) 5172]

Pt has been widely used as a spin current generator and detector in recent novel spin current experiments, e.g.,
spin Seebeck effect,
[Uchida et al., Nature 455, 778 (2008)]
spin pumping,
[Kajiwara et al., Nature 464, 262 (2010)]
spin Hall switching
[Miron et al., Nature 476, 189 (2011)].

III. Giantic spin Hall effect in gold and multi-orbital Kondo effect

Intrinsic spin Hall effect in pure Au

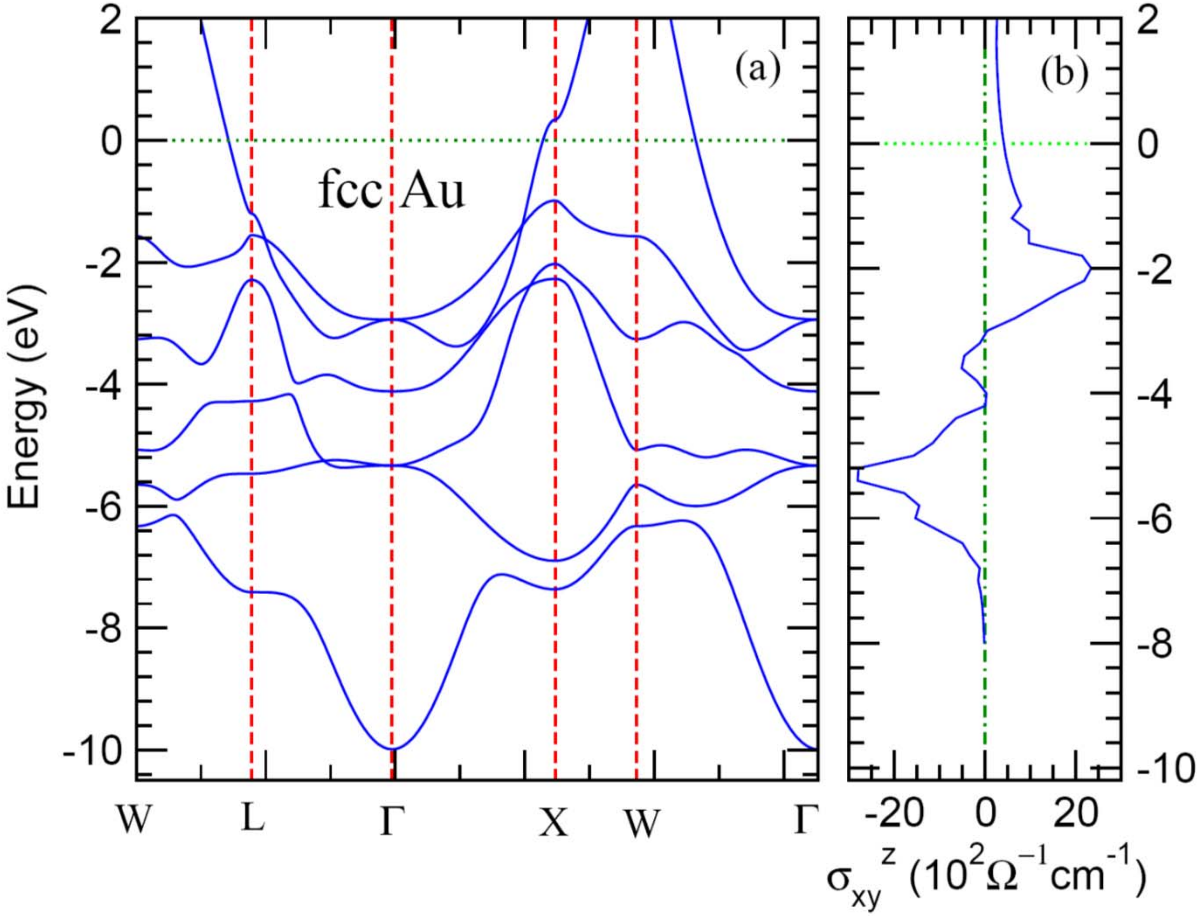

Au: σ_{sH} = 415 $(\Omega cm)^{-1}$ (T = 0 K)
= 750 $(\Omega cm)^{-1}$ (T = 300 K)

[Guo, JAP 105, 07C701 (2009)]

σ_{sH} (exp., RT) = 882 $(\Omega cm)^{-1}$

[Mosendz, et al., PRB 82 (2010) 214403]

1. Giant spin Hall effect in perpendicularly spin-polarized FePt/Au devices

[Seki, et al., Nat. Mater. 7 (2008)125]

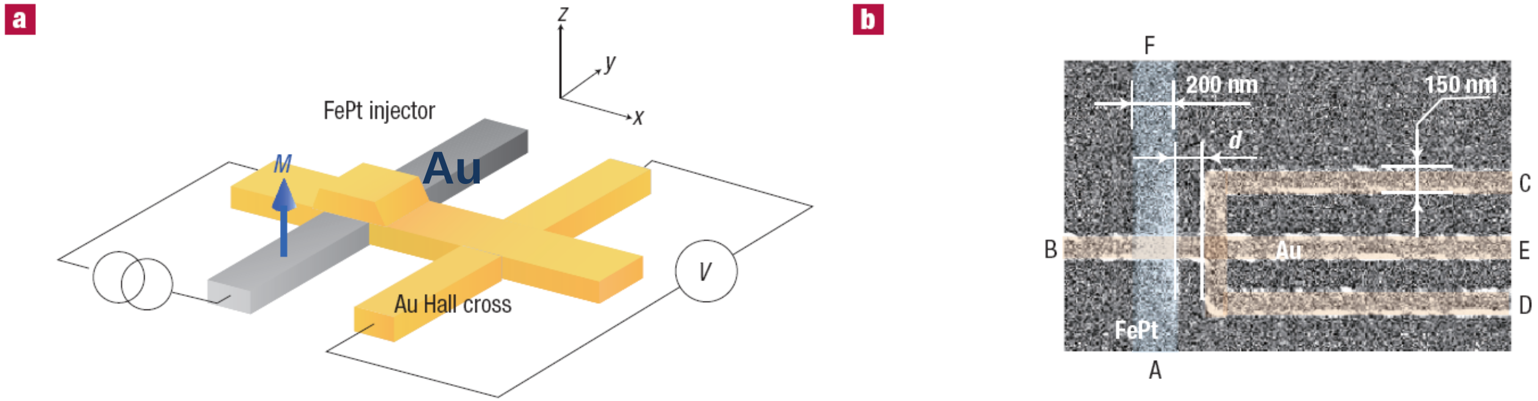

$$\sigma_{sH} \approx 10^5\,\Omega^{-1}\mathrm{cm}^{-1}$$

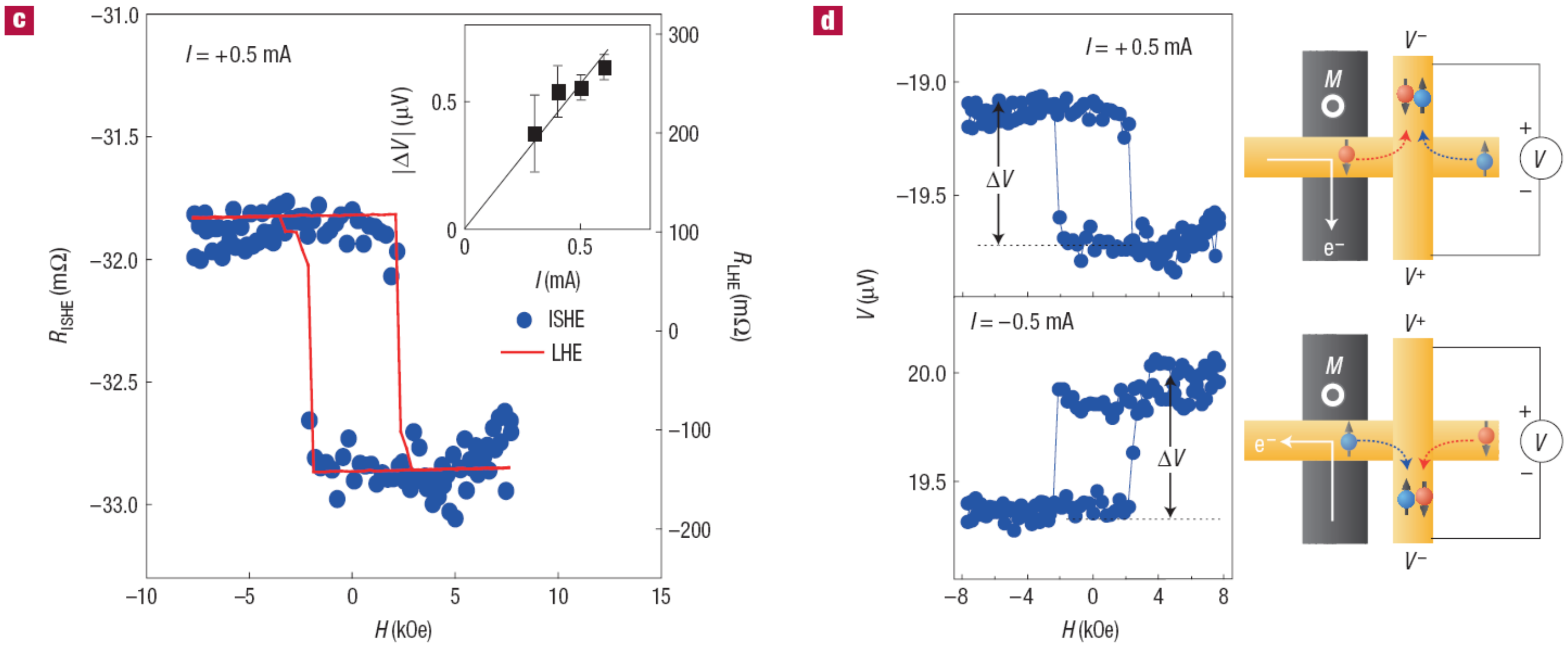

$$\Delta R_{ISHE} = 2\theta_s \frac{\rho_{Au}}{t_{Au}} P \exp(-d/\lambda_{Au}) \quad \text{spin Hall angle} \quad \theta_s = \frac{\sigma_{sH}}{\sigma_{xx}} \approx 0.1 \text{ at RT}$$

What is the origin of giant spin Hall effect in gold Hall bars?

(i) Surface and interface effect? [Seki, et al., Nat. Mater. 7 (2008)125]

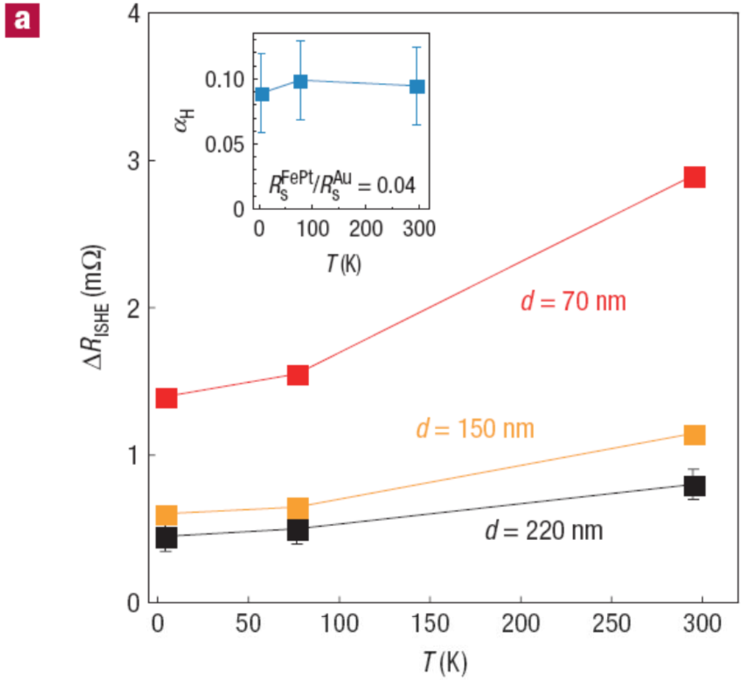

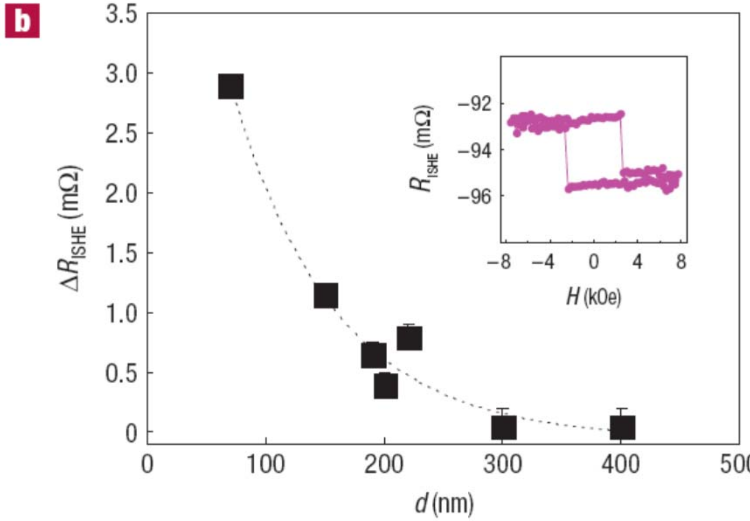

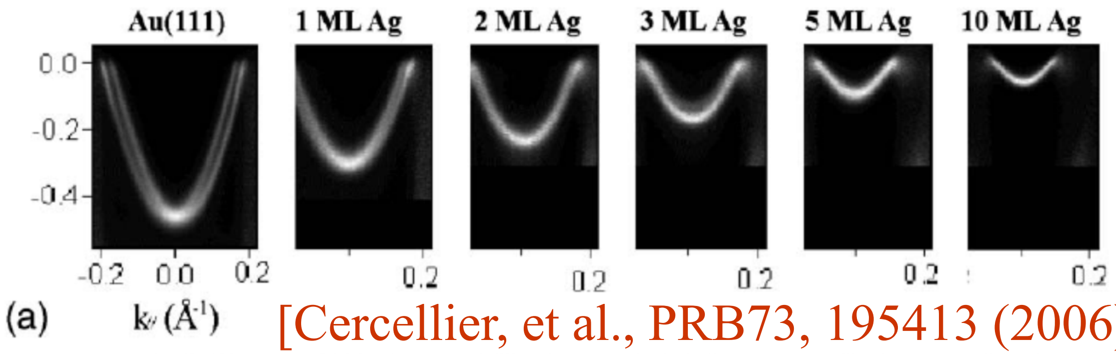

[Cercellier, et al., PRB73, 195413 (2006)]

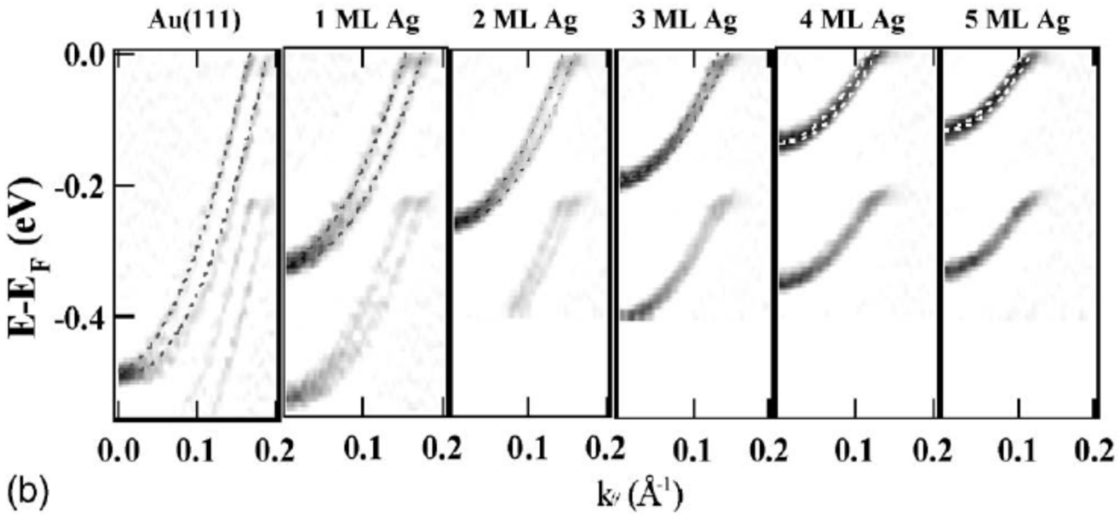

(ii) Defect and impurity origin ?

Possible impurities: (a) vacancy of Au atom
(b) Pt impurity
(c) Fe impurity

2. Spin Hall effect enhanced by multi-orbital Kondo effect

[Guo, Maekawa, Nagaosa, PRL 102, 036401 (2009)]

Results of FLAPW calculations
(a) the change in DOS in the 5d bands.
(b) the DOS change is near -1.5 eV.
Nonmagnetic in (a) and (b)
(c) A peak in DOS at the Fermi level and magnetic.

Proposal: Multiorbital Kondo effect in Fe impurity in gold.

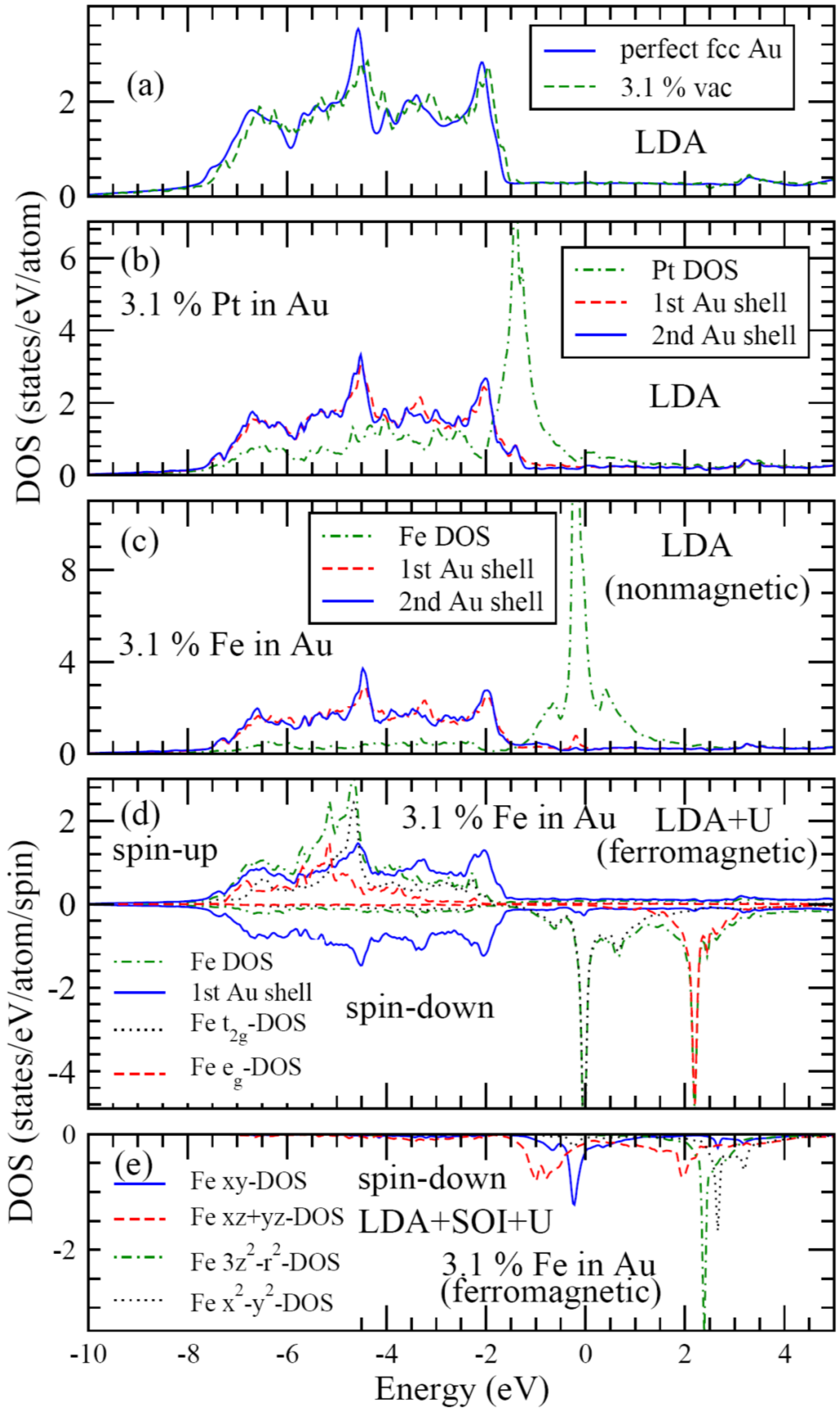

Kondo effect in metals with magnetic impurities

(a classic many-body phenomenon in condensed matter physics)

(1) Resistivity abnormality in Au with dilute magnetic impurities discovered by de Haas et al. in 1930's. [Physica 1 (1934) 1115]

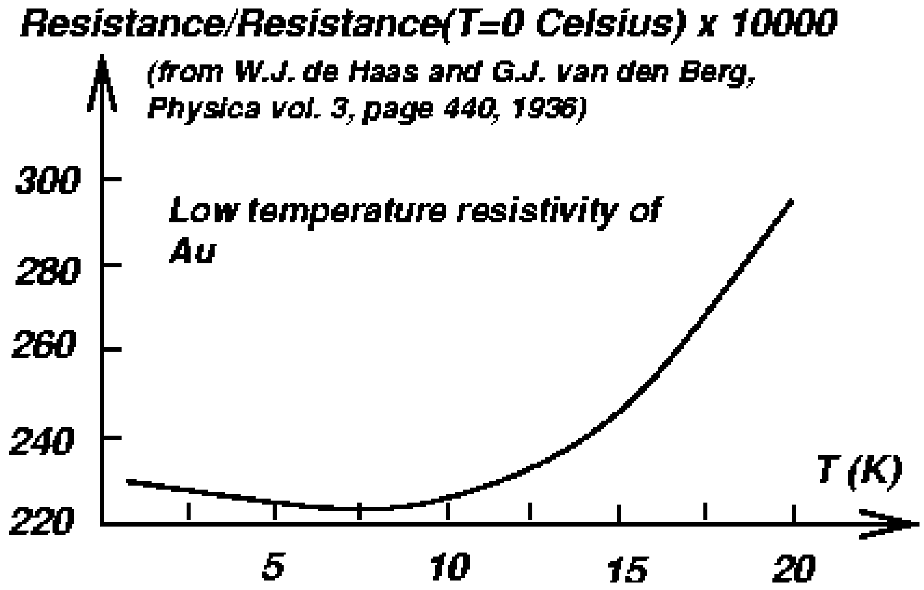

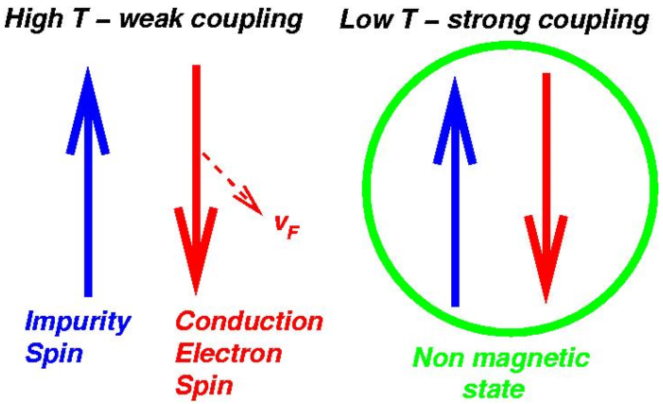

(2) Kondo proposed a (Kondo) model and solved it in the 2nd-order perturbation theory to explain the phenomenon in 1960's. [Prog. Theo. Phys. 32 (1964) 37]

$$H = \sum_{\mathbf{k}\sigma} \varepsilon_k c^\dagger_{\mathbf{k}\sigma} c_{\mathbf{k}\sigma} + J\boldsymbol{\sigma}(0)\cdot\mathbf{S}_f \qquad (J>0,\ S_f = 1/2)$$

$$\rho(T) = aT + C_{imp}\rho_0 - C_{imp}\rho_1 \ln T,$$

$$T_{\min} = (\rho_1/5a)^{1/5} C_{imp}^{1/5} \approx T_K \ \text{(Kondo temperature)}$$

Extrinsic spin Hall effect due to skew scattering

[Guo, Maekawa, Nagaosa, PRL 102, 036401 (2009)]

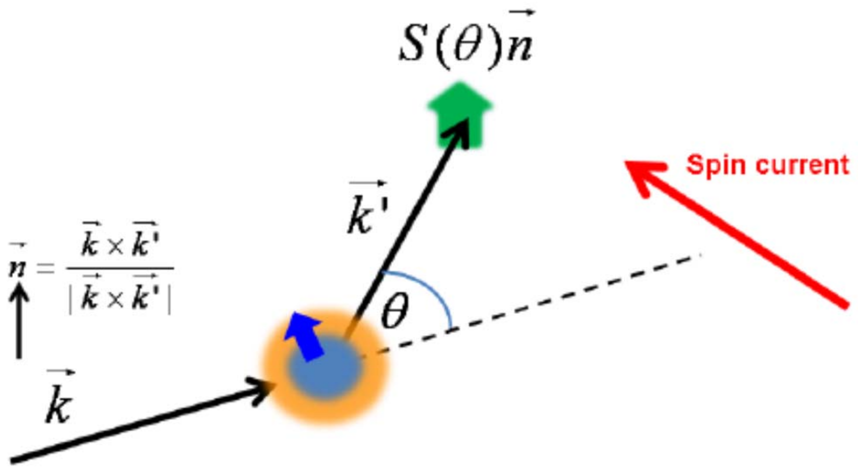

FIG. 1: (color online) The skew scattering due to the spin-orbit interaction of the scatterer and the spin unpolarized electron beam with wavevector $\vec{k}$ with the angle θ with the spin polarization $S(\theta)\vec{n}$ with $\vec{n} = (\vec{k}\times\vec{k}')/|\vec{k}\times\vec{k}'|$.

scattering amplitudes

$$f_\uparrow(\theta) = f_1(\theta)|\uparrow\rangle + ie^{i\varphi}f_2(\theta)|\downarrow\rangle$$
$$f_\downarrow(\theta) = f_1(\theta)|\downarrow\rangle - ie^{-i\varphi}f_2(\theta)|\uparrow\rangle$$

skewness function

$$S(\theta) = \frac{2\mathrm{Im}[f_1^*(\theta)f_2(\theta)]}{|f_1(\theta)|^2 + |f_2(\theta)|^2}$$

spin Hall angle

$$\gamma_S = \frac{\int d\Omega I(\theta)S(\theta)\sin\theta}{\int d\Omega I(\theta)(1-\cos\theta)}$$

$$f_1(\theta) = \sum_l \frac{P_l(\cos\theta)}{2ik}\left[(l+1)\left(e^{2i\delta_l^+}-1\right) + l\left(e^{-2i\delta_l^-}-1\right)\right]$$

$$f_2(\theta) = \sum_l \frac{\sin\theta}{2ik}\left(e^{2i\delta_l^+} - e^{2i\delta_l^-}\right)\frac{d}{d\cos\theta}P_l(\cos\theta).$$

TABLE I. Down-spin occupation numbers of the $3d$ orbitals of the Fe impurity in Au from LDA + U calculations. The calculated magnetic moments are $m_s^{\mathrm{Fe}} = 3.39\mu_B$ and $m_s^{\mathrm{tot}} = 3.32\mu_B$ without SOI, as well as $m_s^{\mathrm{Fe}} = 3.19\mu_B$, $m_o^{\mathrm{Fe}} = 1.54\mu_B$, and $m_s^{\mathrm{tot}} = 3.27\mu_B$ with SOI.

[Guo, Maekawa, Nagaosa, PRL 102, 036401 (2009)]

(a)	xy	xz	yz	$3z^2 - r^2$	$x^2 - y^2$
No SOI	0.459	0.459	0.459	0.053	0.053
SOI	0.559	0.453	0.453	0.050	0.128
(b)	$m = -2$	$m = -1$	$m = 0$	$m = 1$	$m = 2$
No SOI	0.256	0.459	0.053	0.459	0.256
SOI	0.138	0.087	0.050	0.819	0.549

Occupation numbers are related to the phase shifts through generalized Friedel sum rule.

$$\theta_s \cong -\frac{3\delta_1(\cos 2\delta_2^+ - \cos 2\delta_2^-)}{9\sin^2\delta_2^+ + 4\sin^2\delta_2^- + 3[1-\cos 2(\delta_2^+ - \delta_2^-)]}$$

$$\theta_s \cong \delta_1 \approx 0.1$$

$$\theta_H \approx 0.001 \sim 0.01$$

[Fert, et al., JMMM 24 (1981) 231]

Physics 2, 6 (2009)

Piers Coleman
Department of Physics and Astronomy, Rutgers University

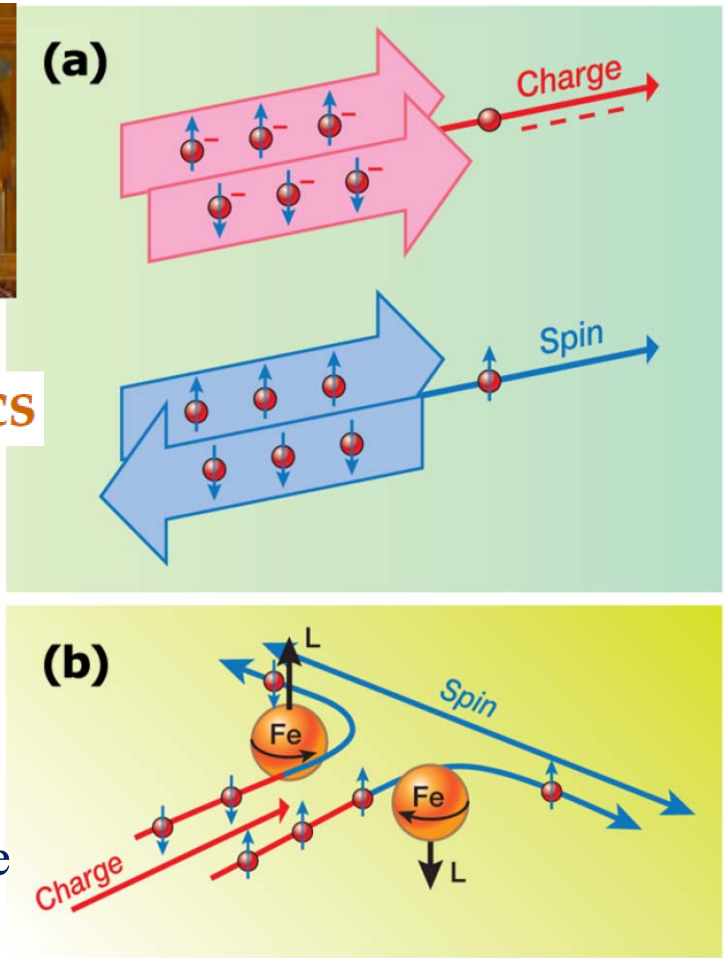

Viewpoint Lending an iron hand to spintronics

In a paper appearing in Physical Review Letters, Guo *et al.*, propose an intriguing theory for this giant spin Hall effect.

Magnetic iron impurities have long been known to have a large effect on the low-*T* resistivity of gold, via the Kondo effect. If Guo *et al.* are right in their interpretation, the observation of a giant spin Hall effect resulting from the Kondo effect will add a curious new twist to this story. The history of the Kondo effect stretches back over seventy-five years. Despite its long history, the detailed Kondo physics of iron remains a controversial subject.

This is a fascinating state of affairs—a wonderful example of the synergy that is possible between electronics applications and condensed-matter physics. If Guo *et al.* are right, the spin Hall conductivity of gold should scale with the iron concentration, moreover, one might expect iron atoms to produce a large anomalous Hall effect. This could be a very exciting and unexpected turn in the long-standing story of the Kondo effect of iron in gold.

A Viewpoint on:
Enhanced Spin Hall Effect by Resonant Skew Scattering in the Orbital-Dependent Kondo Effect
Guang-Yu Guo, Sadamichi Maekawa and Naoto Nagaosa
Phys. Rev. Lett. **102**, 036401 (2009) – Published January 20, 2009

3. Quantum Monte Carlo simulation

1) problems

X-ray magnetic circular dichroism measurements

VOLUME 93, NUMBER 7 PHYSICAL REVIEW LETTERS week ending 13 AUGUST 2004

Direct Observation of Orbital Magnetism in Cubic Solids

W. D. Brewer,[1,*] A. Scherz,[1] C. Sorg,[1] H. Wende,[1] K. Baberschke,[1] P. Bencok,[2] and S. Frota-Pessôa[3]

...t Berlin, Arnimallee 14, D-14195 Berlin-Dahlem, Germany

...ility, BP 220, F-38043 Grenoble Cedex, France

...ulo, CP 66318, 05315-970 São Paulo, São Paulo, Brazil

...2003; published 11 August 2004)

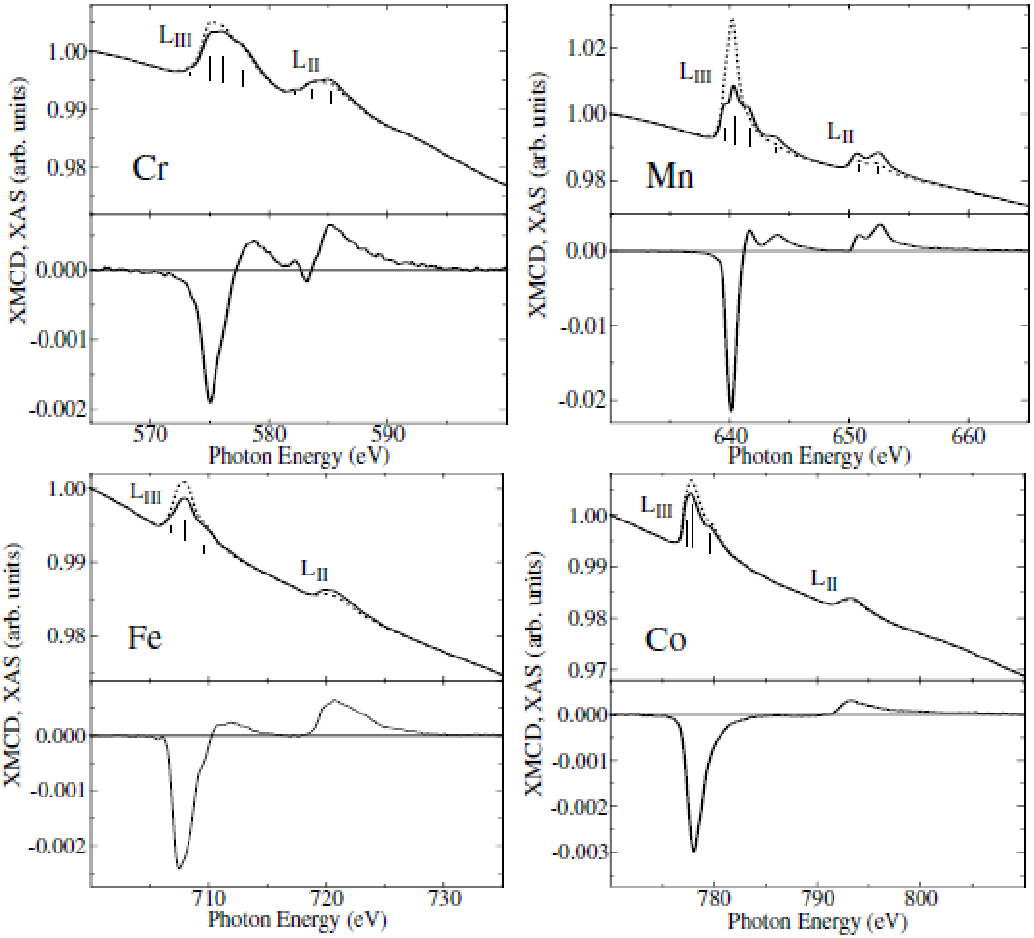

TABLE I. Experimental values of R and the derived orbital/spin magnetic moment ratios for $3d$ impurities in noble metals. The applied field was 7 T, and temperatures T are in K.

Alloy	R	T	$\mu_l/\mu_s^{\mathrm{eff}}$
*Au*Cr (1.0 at. %)	−1.01	18.7	−0.003(30)
*Au*Mn (1.0 at. %)	−0.90	6.8	+0.023(20)
*Cu*Mn (1.0 at. %)	−0.94	6.8	+0.013(20)
*Au*Fe (0.8 at. %)	−0.86	7.2	+0.034(15)
*Au*Co (1.5 at. %)	−0.247	6.8	+0.336(52)

Kondo Decoherence: Finding the Right Spin Model for Iron Impurities in Gold and Silver

T. A. Costi,[1,2] L. Bergqvist,[1] A. Weichselbaum,[3] J. von Delft,[3] T. Micklitz,[4,7] A. Rosch,[4] P. Mavropoulos,[1,2] P. H. Dederichs,[1] F. Mallet,[5] L. Saminadayar,[5,6] and C. Bäuerle[5]

suggests an effective 3-channel Kondo model

$$H = \sum_{k\alpha\alpha} \varepsilon_k c^\dagger_{k\alpha\sigma} c_{k\alpha\sigma} + J \sum_{\alpha} \mathbf{S} \cdot \mathbf{s}_\alpha.$$

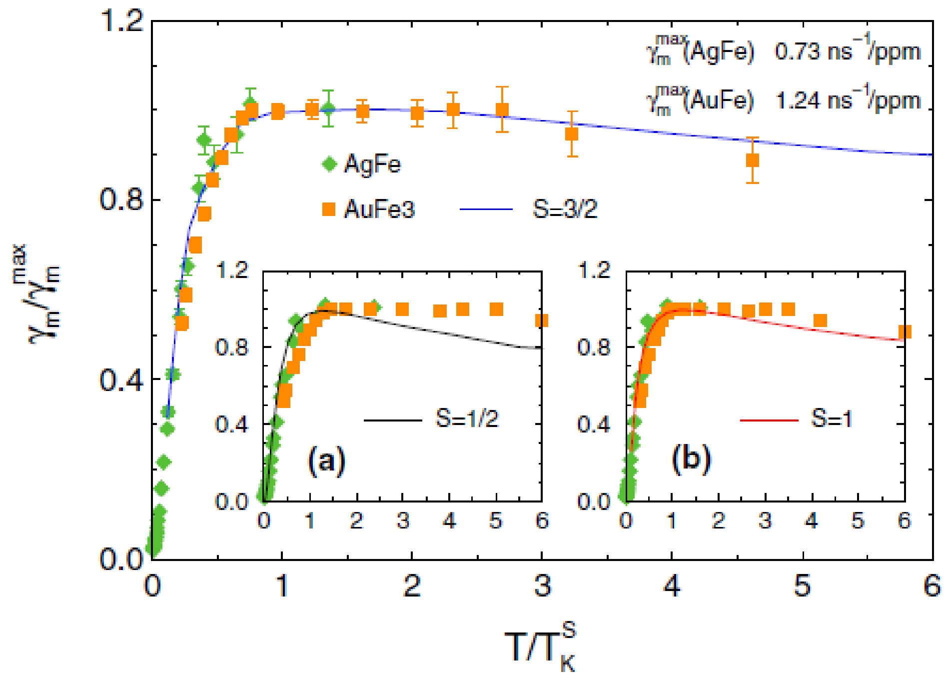

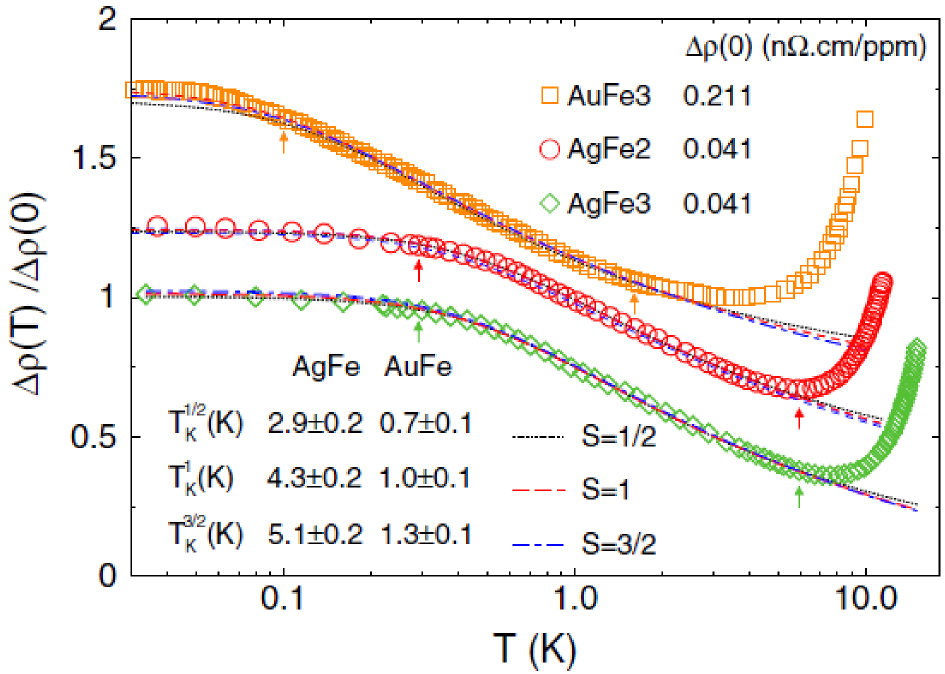

2) Quantum Monte Carlo simulation

[Gu, Gan, Bulut, Ziman, Guo, Nagaosa, Maekawa, PRL105 (2010) 086401]

(1) Single-impurity multi-orbital Anderson Model

A realistic Anderson model is formulated with the host band structure and the impurity-host hybridization determined by ab initio DFT-LDA calculations.

$$H = \sum_{\alpha,k,\sigma} \varepsilon_{\alpha k} c^{+}_{\alpha k \sigma} c_{\alpha k \sigma} + \sum_{\xi,\sigma} \varepsilon_{\xi} d^{+}_{\xi\sigma} d_{\xi\sigma} + \sum_{\alpha,k,\xi,\sigma} \left(V_{\alpha k \xi} c^{+}_{\alpha k \sigma} d_{\xi\sigma} + h.c. \right)$$

$$+ U \sum_{\xi} n_{\xi\uparrow} n_{\xi\downarrow} + U' \sum_{\sigma,\sigma'} n_{1\sigma} n_{2\sigma'} - J \sum_{\sigma} n_{1\sigma} n_{2\sigma}$$

For host band structure, α = 9 bands (6s, 6p, 5d orbitals of Au) are included.
For impurity-host hybridization, $Au_{26}Fe$ supercell (3X3X3 primitive FCC cell) is considered. $\xi = 5$ (3d orbitals of Fe).

For impurity Fe, one e_g orbital (z^2) and one t_{2g} orbital (xz) are considered with the following parameters.

U = 5 eV, J = 0.9 eV, U'= U – 2J = 3.2 eV

(2) Magnetic behaviors for Fe in Au from QMC simulations

[Gu, Gan, Bulut, Ziman, Guo, Nagaosa, Maekawa, PRL105 (2010) 086401]

3-Orbitals case

$$\xi = 1 : z^2,$$

$$\xi = 2 : -\frac{1}{\sqrt{2}}(xz - iyz) : p_1 : l = 1, m = 1;$$

$$\xi = 3 : -\frac{1}{\sqrt{2}}(xz + iyz) : p_{-1} : l = 1, m = -1.$$

Local moment

$$M_\xi^z = n_{\xi\uparrow} - n_{\xi\downarrow},$$

Impurity magnetic susceptibility

$$\chi_\xi = \int_0^\beta d\tau \langle M_\xi^z(\tau) M_\xi^z(0) \rangle,$$

Occupation number

$$n_\xi = n_{\xi\uparrow} + n_{\xi\downarrow},$$

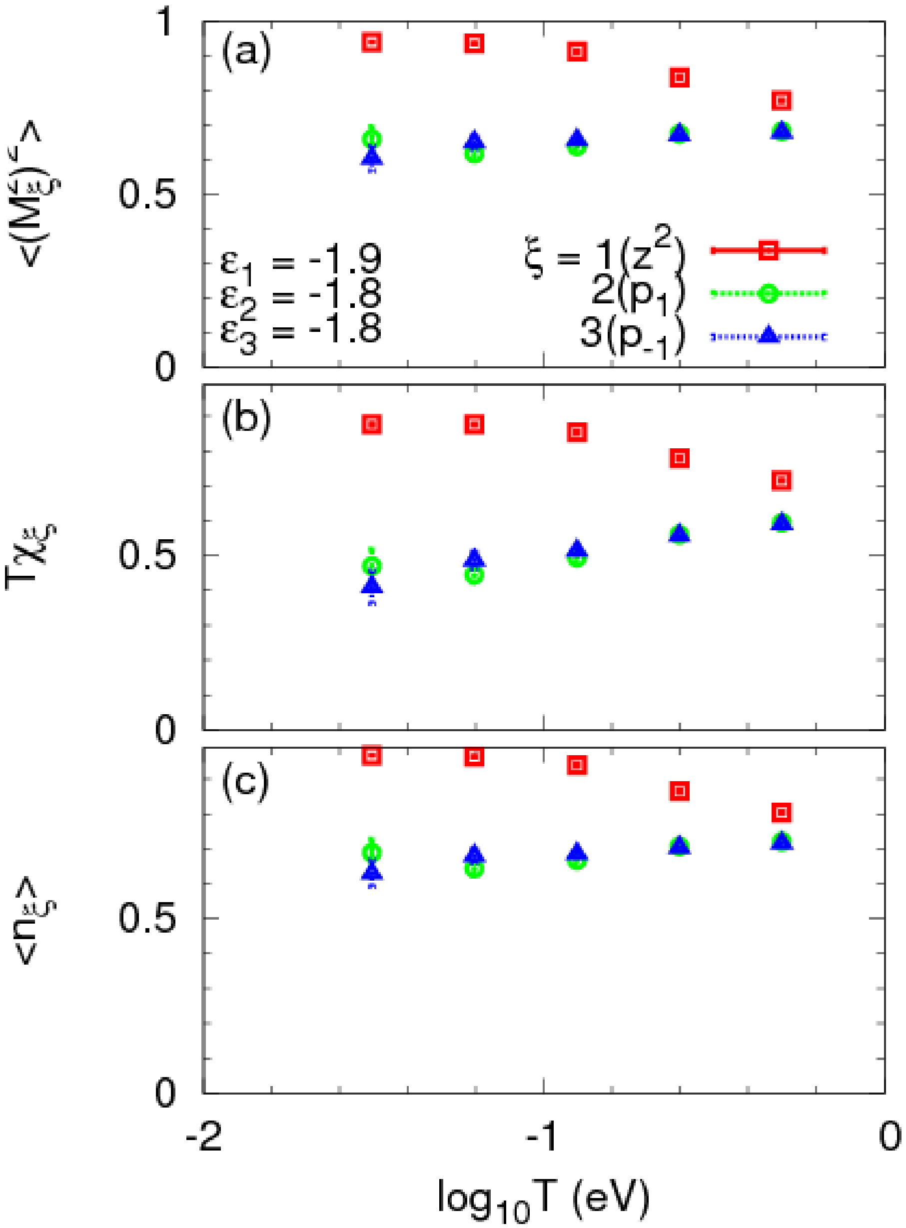

(3) Spin-orbit interaction within t_{2g} oribtals for Fe in Au

[Gu, Gan, Bulut, Ziman, Guo, Nagaosa, Maekawa, PRL105 (2010) 086401]

Ising-type spin-orbit interaction for *p*-electrons: l =1, m =1,0,-1.

$$H_{so} = (\lambda/2) \sum_{m,m',\sigma,\sigma'} d^{\dagger}_{m\sigma} (\mathbf{l})_{mm'} \cdot (\sigma)_{\sigma\sigma'} d_{m'\sigma'} ,$$

$$H_{so} = (\lambda/2) \sum_{m,\sigma} d^{\dagger}_{m\sigma} (\mathbf{l})^z_{mm} (\sigma)^z_{\sigma\sigma} d_{m\sigma} .$$

$$l^z = \begin{pmatrix} 1 & 0 & 0 \\ 0 & 0 & 0 \\ 0 & 0 & -1 \end{pmatrix}, \sigma^z = \begin{pmatrix} 1 & 0 \\ 0 & -1 \end{pmatrix},$$

$$H_{so} = (\lambda/2) \left(n_{1\uparrow} - n_{1\downarrow} - n_{-1\uparrow} + n_{-1\downarrow} \right) ,$$

T = 350 K, = 75 meV

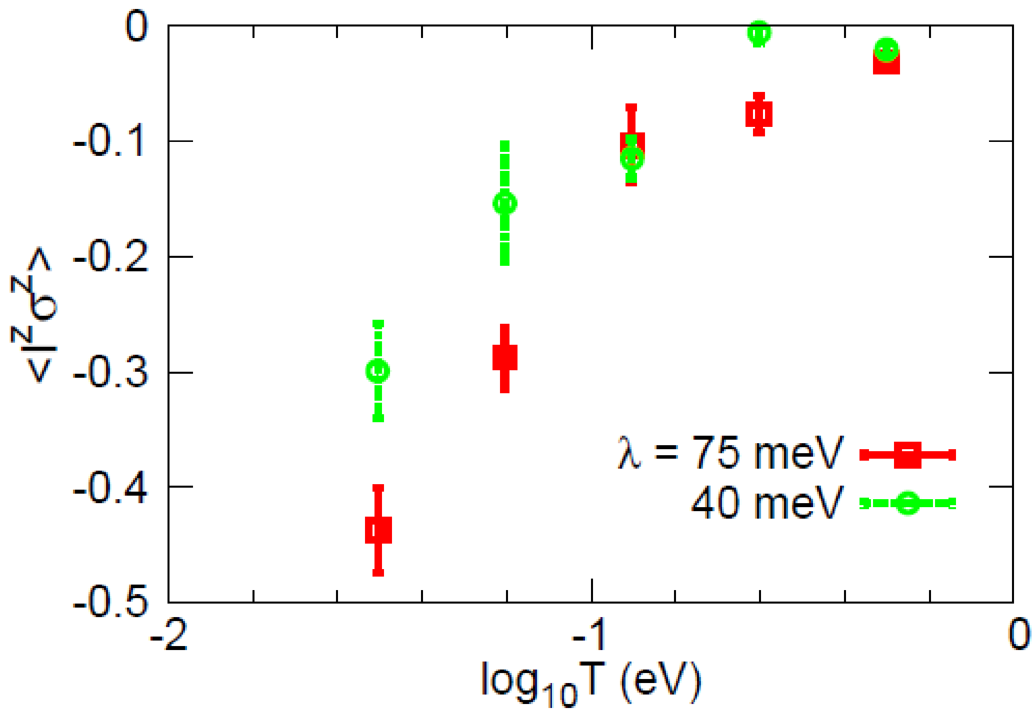

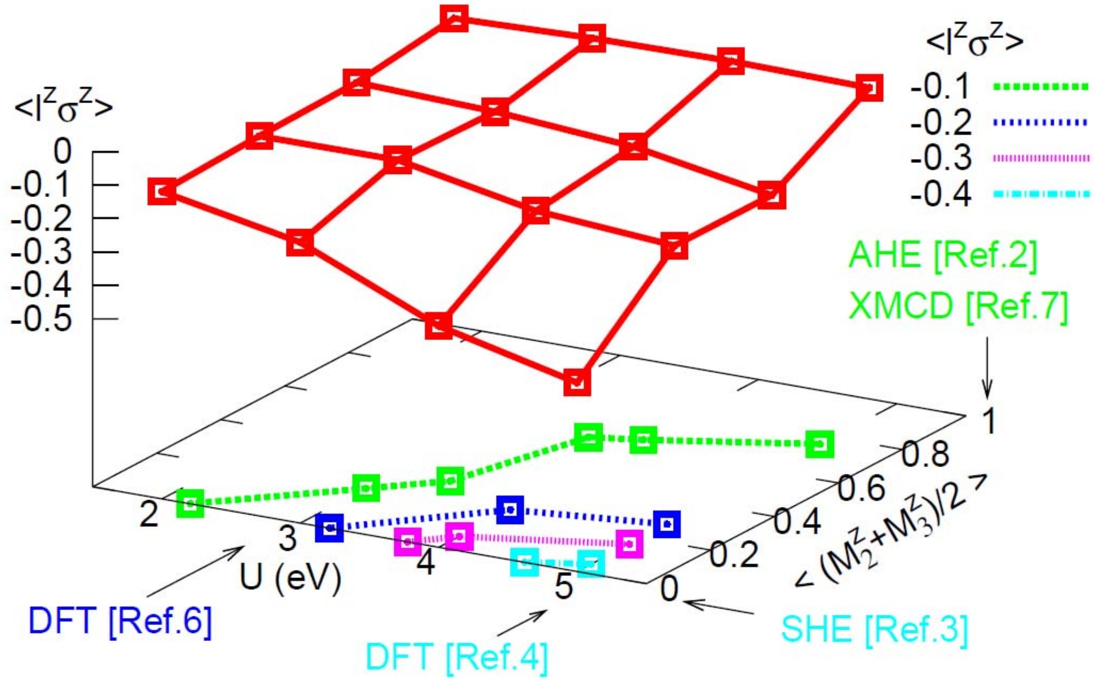

(4) Estimation of spin Hall angle for Fe impurity in Au

$$\gamma_s \cong -\frac{3\delta_1(\cos 2\delta_2^+ - \cos 2\delta_2^-)}{9\sin^2\delta_2^+ + 4\sin^2\delta_2^- + 3[1-\cos 2(\delta_2^+ - \delta_2^-)]}$$

Since we consider only two t_{2g} orbitals with $\ell_z = \pm 1$, the SOI within the t_{2g} orbitals gives rise to the difference in the occupation numbers between the parallel (n_P) and anti-parallel (n_{AP}) states of the spin and angular momenta. These occupation numbers are related to the phase shifts δ_P and δ_{AP}, through generalized Friedel sum rule, respectively, as $n_{P(AP)} = \delta_{P(AP)}/\pi$, and $\pi < \ell_z\sigma_z > = \delta_P - \delta_{AP}$, $\pi < n_2 > = \pi < n_3 > = \delta_P + \delta_{AP}$.

Putting $< \ell_z\sigma_z > = -0.44$ for $\lambda = 75$ meV, and $< n_2 > = < n_3 > = 0.65$, we obtain $\delta_P = 1.35$ and $\delta_{AP} = 2.73$.

Taking into account the estimate $\sin \delta_1 \sim= 0.1$, $\gamma_s \sim= 0.06$ is thus obtained.

[Seki, et al., Nat. Mater. 7 (2008)125]

$\gamma_s \sim= 0.11$ (exp.)

Influence of Fe Impurity on Spin Hall Effect in Au

Isamu Sugai[1], Seiji Mitani[2], and Koki Takanashi[1]

[1]Institute for Materials Research, Tohoku University, Sendai 980-8577, Japan
[2]National Institute for Materials Science, Tsukuba 305-0047, Japan

We investigated the influence of Fe impurity on spin Hall effect in Au using multi-terminal devices consisting of an FePt perpendicular spin polarizer and a Au Hall cross with different Fe impurity concentrations. As the Fe impurity concentration was increased in the range of 0–0.95 at.%, the resistivity of Au doped with Fe increased and the spin diffusion length decreased from 35 nm to 27 nm. On the other hand, the spin Hall angle for Au doped with Fe, evaluated from the spin injector-Hall cross distance dependence of spin Hall signals, was approximately 0.07, independent of the Fe concentration. The experimental results provide important information for understanding the mechanism of the large spin Hall effect.

Skew scattering
θ_s ~0.07 ,
independent of
Fe concentration.

PARAMETERS OF $P_{\underline{\mathrm{Au}}\mathrm{Fe}}$, $R_s^{\underline{\mathrm{Au}}\mathrm{Fe}}$, $\lambda_{\underline{\mathrm{Au}}\mathrm{Fe}}$, P AND α_H OBTAINED FOR THE PRESENT FePt/Au DEVICES

	$\rho_{\underline{\mathrm{Au}}\mathrm{Fe}}$ [μΩ·cm]	$\lambda_{\underline{\mathrm{Au}}\mathrm{Fe}}$ [nm]	$R_s^{\underline{\mathrm{Au}}\mathrm{Fe}}$ [Ω]	P	α_H
Non-doped Au	3.6	35 ± 4	1.1	0.038	0.07 ± 0.02
$Au_{99.58}Fe_{0.42}$	4.3	33 ± 3	1.3	0.034	0.07 ± 0.01
$Au_{99.05}Fe_{0.95}$	7.0	27 ± 3	1.7	0.027	0.07 ± 0.03

IV. Summary

1. Spin Hall effect, a manifestation of special relativity, is rich of fundamental physics, and is related to such classic phenomena in condensed matter physics as Kondo effect.

2. Spin Hall effect may be used to generate, detect and manipulate spin currents, and hence has important applications in spintronics and magneto-devices.

3. *Ab initio* band theoretical calculations not only play an important role in revealing the mechanism of spin Hall effect, but also help in searching for and designing new spintronic materials.

4. Recent intensive research on spin Hall effect has also led to the creation of such hot fields such as topological insulators and spin caloritronics.

Acknowledgements:

Discussions and Collaborations:

Qian Niu (UT Austin & PKU), Yugui Yao (BIT)
Tsung-Wei Chen (Nat'l Sun Yat-sen U.)
Yang-Fang Chen and his experimental team (Taida)
Naoto Nagaosa (Tokyo U.)
Shuichi Murakami (Tokyo Inst. Techno.)
Bo Gu, Sadamichi Maekawa (JAEA)

Financial Support:

National Science Council of The R.O.C.